58pp.

NASA TM X-1109

AN AIRFOIL SHAPE FOR EFFICIENT FLIGHT AT SUPERCRITICAL MACH NUMBERS

By Richard T. Whitcomb and Larry R. Clark

Langley Research Center
Langley Station, Hampton, Va.

NATIONAL AERONAUTICS AND SPACE ADMINISTRATION

AN AIRFOIL SHAPE FOR EFFICIENT FLIGHT AT SUPERCRITICAL MACH NUMBERS*

By Richard T. Whitcomb and Larry R. Clark
Langley Research Center

SUMMARY

An airfoil shape is proposed for delaying, at the usual cruise lift conditions, the subsonic drag rise well beyond the critical Mach number. The shape has a slot between the upper and lower surfaces near the trailing edge to delay shock-induced separation on both surfaces and incorporates negative camber ahead of the slot with substantial positive camber rearward of the slot to reduce shock losses. Wind-tunnel results obtained at Mach numbers from 0.65 to 0.80 for two-dimensional models of a 13.5-percent-thick airfoil of the proposed shape and an NACA 64A-series airfoil, used as a base of reference, indicate that for the design-section normal-force coefficient of 0.65 the proposed shape has a drag rise at a Mach number of 0.79 compared with a drag-rise Mach number of 0.67 for the NACA 64A-series airfoil. The drag at a Mach number just less than that of drag rise for the proposed airfoil is due almost entirely to skin friction and is approximately 10 percent greater than that for the 64A-series airfoil. The section pitching-moment coefficient for the proposed shape is substantially more negative than that for conventional airfoils. The proposed airfoil shape also significantly increases the stall section normal-force coefficient at high subsonic speeds.

INTRODUCTION

It is generally recognized that the operating economics of aircraft intended to cruise at high subsonic speeds can usually be substantially improved by delaying the drag rise associated with the development of local supersonic flow on the upper surface of the wing. Numerous methods have been proposed to postpone this drag rise. (See ref. 1.) The fundamental approach for a number of such techniques has been to delay the onset of effective supersonic Mach numbers, that is, to delay the critical Mach number. Among these methods are the use of thinner airfoil sections, sweepback, and area ruling, including antishock bodies. Another approach has been to eliminate shock-induced separation even with local supersonic flow present, that is, at supercritical Mach numbers. Techniques to accomplish the latter approach include special camber distributions, vortex generators, and the injection of high-energy air into the boundary layer near the shock wave. Each of the methods of both approaches has

certain inherent disadvantages which offset partially or wholly the favorable actions of the system; for example, sweepback reduces the aerodynamic aspect ratio for a given structural aspect ratio, decreases the usable lift coefficient at landing conditions, and may lead to the well-known pitch-up condition, while boundary-layer injection requires an additional input of energy and a complex piping arrangement. For this latter system, the magnitude of these disadvantages has precluded its use on an actual airplane.

In the technique described herein, the objective has been to delay the drag rise for the usual cruise lift conditions well beyond the critical Mach number by specially shaping the airfoil, including the insertion of a slot between the lower and upper surfaces. This airfoil modification should delay drag rise by a substantially greater increment than the previously proposed shape changes. Further, the proposed method should have a number of advantages over the various previous techniques for delaying drag rise. The present paper includes a discussion of the aerodynamic factors involved in the proposed approach with substantiating results obtained for two-dimensional airfoil models in the Langley 8-foot transonic pressure tunnel.

Experimental results have been obtained for a number of variations of the proposed airfoil. However, to expedite publication, the major portion of the results presented herein has been limited to those for the most successful configuration. For this particular configuration, experimental results were obtained only at near-design conditions. To provide an indication of the general effect of the proposed concept at off-design conditions, results are included for a configuration which differed somewhat from the most successful version in both shape and the transition-strip arrangement.

SYMBOLS

c_d section drag coefficient, $\sum \frac{c_{d'} \Delta z'}{c}$

$c_{d'}$ point drag coefficient

c_m section pitching-moment coefficient,

$$\sum_{l.s.} \frac{c_p \Delta x}{c}\left(0.25 - \frac{x}{c}\right) - \sum_{u.s.} \frac{c_p \Delta x}{c}\left(0.25 - \frac{x}{c}\right)$$

or $$\int_{l.s.} c_p\left(0.25 - \frac{x}{c}\right)d\left(\frac{x}{c}\right) - \int_{u.s.} c_p\left(0.25 - \frac{x}{c}\right)d\left(\frac{x}{c}\right)$$

c_n section normal-force coefficient, $\sum_{l.s.} \frac{c_p \Delta x}{c} - \sum_{u.s.} \frac{c_p \Delta x}{c}$

C_p	pressure coefficient, $\left(\frac{p - p_o}{q}\right)$
$C_{p,sonic}$	pressure coefficient corresponding to local Mach number of 1.0
c	chord of airfoil, in. (cm)
M	Mach number
p	local static pressure at a point on the airfoil, lb/ft^2 (newton/meter^2)
p_o	static pressure in undisturbed stream, lb/ft^2 (newton/meter^2)
Δp_t	total-pressure loss, lb/ft^2 (newton/meter^2)
q	dynamic pressure in undisturbed stream, lb/ft^2 (newton/meter^2)
t	airfoil thickness, in. (cm)
V	velocity in undisturbed stream, ft/sec (meter/second)
x	ordinate along airfoil reference line measured from airfoil leading edge, in. (cm) unless otherwise stated
z	ordinate vertical to airfoil reference line, in. (cm) unless otherwise stated
z'	vertical distance in wake profile, in. (cm)
α	angle of attack of airfoil reference line, deg

Subscripts:

l.s.	lower surface
u.s.	upper surface

BASIC CONCEPTS

It is well known that at even moderate supercritical Mach numbers, a broad local region of supersonic flow extends vertically from an airfoil. (See fig. 1.) This region is usually terminated by a shock wave which, of course, directly causes an energy loss and thus a drag increase. More importantly, the shock produces a positive pressure gradient at the surface of the airfoil which may be sufficiently great to cause separation of the boundary layer with an associated large drag increase. At lifting conditions, supercritical flow

usually develops first on the upper surface. However, such a flow also occurs on the lower surface at higher Mach numbers.

For the airfoil shape proposed herein (fig. 2(a)), a slot between the upper and lower surface is intended to reduce the possibility of shock-induced separation on both surfaces while negative camber on the forward portion of the airfoil with substantial positive camber in the rearward part is intended to reduce the shock-wave losses above the upper surface. The rationale leading to this shape is summarized briefly in this section.

Throughout the paper, this proposed airfoil shape will be referred to as the supercritical airfoil. The portions of the shape forward of and rearward of the slot will be called the fore and aft components, respectively.

Reduction of Tendency Toward Boundary-Layer Separation

Upper surface.- Fundamentally, shock-induced separation occurs initially on an airfoil because the low-momentum boundary layer cannot traverse the pressure rise through the shock wave superimposed on the subcritical pressure recovery (fig. 1). In the present approach, the slot introduces stream energy air under the upper-surface boundary layer at an intermediate point of the combined pressure rise. With such an arrangement, the boundary layer on the upper surface of the fore component moves through the part of the pressure rise ahead of the slot exit in the normal manner, then, with the boundary layer of the lower surface of the fore component, traverses the remaining rise behind the slot as an unconfined wake. Theory and experiment have shown that the rate of momentum transfer in a wake is substantially greater than in a turbulent boundary layer. As a result, for the present device, the energy of the wake at the end of the pressure rise over the aft component is substantially increased, and the wake can traverse a total pressure rise without reversal significantly greater than could a confined boundary layer. Also, with the shock wave ahead of the slot, the tendency toward separation for the new boundary layer on the aft component, in the part of the pressure rise on that component, can be made relatively low if this aft component is shaped to provide a pressure rise of reasonable slope.

When the shock moves rearward of the slot exit, the boundary layer on the aft component is required to traverse the complete pressure rise of the system. For such a condition, the tendency for this boundary layer to separate is greatly increased.

The action of the proposed device should be quite similar to that of the slot used in combination with a flap to achieve greater low-speed lift without separation. Also, the effect of the slot should be the same as that of injecting high-energy air under the boundary layer as previously investigated. (See ref. 1.) However, with the presently proposed method, the effect would be accomplished without the need for additional energy or complex ducting.

Lower surface.- With the possible delay of the onset of shock-induced boundary-layer separation on the upper surface provided by the action of the

slot, the initial development of such separation may occur on the lower surface, particularly for an airfoil incorporating the shape changes intended to reduce shock losses, as described in the next section.

Interposition of the slot entrance at an intermediate point in the pressure rise along the aft portion of the lower surface should reduce the tendency toward boundary-layer separation on that surface through an action closely related to the proposed effect of the slot on the upper-surface flow. With such an arrangement, the boundary layer on the fore component is required to traverse only the part of the pressure rise ahead of the slot entrance before moving into the slot where a decreasing favorable pressure gradient can be provided because of the diminished pressure at the exit of the slot. Further, the tendency toward separation for the new boundary layer on the aft component in the part of the pressure rise on that surface should be very low.

The effect of the slot on the lower-surface boundary-layer flow should be similar to that of boundary-layer suction previously investigated (ref. 1). Again, for the present airfoil, the action would be accomplished without the need for additional energy or complex ducting.

Reduction of Shock Losses

At the usual cruise lift coefficients and for Mach numbers below the probable final abrupt drag rise of the proposed supercritical airfoil, the losses associated with any shock wave below the lower surface should be relatively small. Therefore, for the present case, the primary concern has been to reduce shock losses above the upper surface.

Modification of camber distribution.- If shock-induced separation is eliminated, the shock wave moves rearward with a usual increase in the Mach number ahead of the shock and an increase in the vertical extent of the wave. As a result, the energy losses associated with the shock increase substantially. While the resulting increase in drag is usually significantly less than that due to separation, for an airplane intended to cruise at subsonic speeds any increase is undesirable.

Obviously, the shock losses can be diminished by reducing the vertical extent of the supersonic region and the terminating shock wave and diminishing the supersonic Mach numbers ahead of the wave. The accomplishment of such an objective also retards the rearward movement of the shock with increasing free-stream Mach number and this, with the presently proposed arrangement, delays the Mach number at which the shock moves aft of the slot exit with an associated large increase in the tendency toward separation on the upper surface of the aft component. These effects can be accomplished by reducing the curvature and slope of the upper surface ahead of the shock.

The reduction in camber associated with a diminished curvature of the upper surface, of course, results in a reduction of the lift carried by the middle region of the airfoil. This lift must be recovered elsewhere. A part of the additional lift required can be achieved by increasing the load carried by the

forward region of the fore component through an increase of the incidence of that region as described in reference 1. However, such a change leads to adverse effects at off-design, high-lift conditions so that its application for the design condition must be limited. In the present approach, the major part of the required additional lift is carried on the region of the airfoil behind the shock position, particularly on the lower surface. The increase of lift in this area is achieved by substantial positive camber and incidence of the aft region of the airfoil, especially of the lower surface.

The favorable effects on the drag rise of more negative camber in the forward region of the airfoil or more positive camber on the rearward portion have been noted by several previous investigators. (See ref. 1, for example.)

Influence of the slot.- The use of the camber changes to reduce shock losses as previously described results in substantial increases in the tendency toward boundary-layer separation on both the upper and lower surfaces. On the upper surface, the pressure-recovery gradient is increased near the trailing edge. On the lower surface, the induced velocities in the middle region of the surface are increased with a resulting earlier development of a region of supersonic flow and an associated shock wave. Also, the pressure-recovery gradient on the lower surface is exaggerated in the region of the reflex of the camber modification. Obviously, these adverse effects limit the magnitude of the camber modifications which may be incorporated without causing undesirable separation on the airfoil.

The effects of the slot should significantly reduce these increased tendencies toward separation associated with the camber modifications. As a result, the presence of the slot should allow an increase in the magnitude of these modifications that can be utilized without the development of separation.

DEVELOPMENT OF DETAILED SHAPE

Several groups in this country are now developing procedures based on the characteristics method for defining airfoil shapes to achieve desired pressure distributions for the condition of interest here, that is, for subsonic stream Mach numbers but with a large region of supersonic flow present. However, at the present time, none of the work has fully accomplished this objective. In the present approach, the detailed shape of the airfoil was arrived at on the basis of intuitive reasoning and substantiating experiment.

In the detailed shaping of the airfoil the objectives have been: first, to eliminate boundary-layer separation on both the upper and lower surfaces at the design-section normal-force coefficient for Mach numbers below that at which the shock above the upper surface moves rearward of the slot exit; second, to delay to the highest Mach number possible this movement of the shock rearward of the slot exit which, as preliminary experiments indicate, causes an abrupt, uncontrollable drag rise; third, to reduce the shock losses above the upper surface to a minimum at a Mach number just below that of the abrupt drag rise; fourth, to provide satisfactory characteristics at off-design conditions; and

finally, to minimize the added skin-friction losses of the proposed airfoil. Since the general shape changes required to achieve various objectives are, in several instances, directly contradictory, the total shape must be a compromise.

Fore Component

Upper surface.- The tendency toward boundary-layer separation on the upper surface of the fore component at supercritical conditions should be minimized by limiting the pressure rise on this surface to approximately that of the shock wave. (See fig. 1.) This effect is accomplished by providing a relatively small surface slope in the rearward part of the upper surface of the fore component and incorporating the proper curvature in this region of the fore component and the upper surface of the aft component.

Considerable experimental research has been performed by several groups (ref. 1, for example) to develop airfoil shapes which achieve reduced strength of the upper-surface shock wave at lifting conditions for Mach numbers at which the shock wave is above the forward region of the airfoil. However, for the condition selected to minimize the shock losses of the present configuration, that is, at a Mach number just below the abrupt drag rise, the shock wave will be well rearward on the fore component, normally just ahead of the slot exit. Thus, the results of the previous work, while helpful in providing certain insights, are not directly applicable to determining the most satisfactory upper-surface shape for the proposed supercritical airfoil.

For the present configuration, the extent of the shock wave has been reduced primarily by shaping the upper surface of the fore component to provide a local supersonic field similar in shape to that shown in figure 1. This field expands to a maximum above the middle region of the fore component and then contracts between this region and the shock wave. An excessively rapid rate of contraction of the supersonic field results in a close concentration of positive disturbances near the surface. These may converge with a resulting increase in the strength of the remaining shock wave, particularly at off-design conditions. Thus, the contraction must be limited to a reasonably noncritical rate. Further reduction of the extent of the shock must be accomplished by shaping the airfoil to provide a reduced maximum extent of the supersonic field. Also, the losses in the wave can be diminished by reducing the Mach numbers near the surface just ahead of the shock wave. These several objectives have been achieved by the use of relatively small, roughly uniform, surface curvature and near zero mean slope for a broad region extending from somewhat rearward of the leading edge (approximately 0.15c) to the probable shock position (approximately 0.75c). The crest line, or maximum vertical penetration of the surface, is near the middle of this region (approximately 0.45c).

As noted in the preceding section entitled "Basic Concepts," these shape changes should also delay to higher Mach numbers the movement of the shock wave rearward of the slot exit.

The curvature of the upper surface of the fore component of the airfoil of figure 2(a) is greater than that required to obtain the maximum reduction of

shock losses and retardation of the rearward movement of the shock wave. This greater than optimum curvature has been incorporated arbitrarily in order to limit the curvature of the lower surface of the fore component with its associated adverse effect on the tendency toward boundary-layer separation.

For the configuration shown in figure 2(a), the shape of the extreme forward part of the fore component has been designed to minimize the induced-pressure peaks at subcritical high-lift conditions.

Lower surface.- The preliminary experiments of this program have indicated that the onset of boundary-layer separation on the lower surface of the fore component destroys the effectiveness of the slot in controlling separation on the upper surface with a resulting severe loss in lift. Therefore, it is imperative that such separation be delayed to a Mach number higher than that for the abrupt drag rise associated with movement of the upper-surface shock rearward of the slot exit. While the action of the slot substantially reduces the tendency toward separation, additional refinements must be incorporated in the shape of this surface to allow the use of substantial negative camber in the fore component and still assure the required delay of separation.

To reduce the magnitude of the maximum induced velocities on the lower surface of the fore component and thus delay the onset of supercritical flow and the associated shock wave, this surface should be shaped to provide an extensive region of roughly constant induced negative pressure similar to that on the NACA 16-series airfoil.

To reduce the tendency toward separation of the boundary layer in the pressure-recovery region along the aft portion of the lower surface of the fore component, the magnitude of this recovery should be minimized to that required to reach the pressure at the entrance to the slot, that is, by eliminating any overcompression. (See fig. 1.) To provide such a limited pressure rise in the presence of the large positive pressures associated with the aft component requires a substantial convex curvature of the surface similar to that shown in figure 2(a).

Aft Component

Upper surface.- For relatively high design lift coefficients, at least, the most effective airfoil shape should probably be achieved by designing the aft component to produce the greatest increment in lift within the limitation imposed by boundary-layer separation on the upper surface of this component and the requirement for structural integrity. Results of the preliminary unreported experiments of this program indicate that boundary-layer separation on the upper surface can be avoided if the upper surface is shaped to provide a reasonable pressure recovery and to produce no more than slightly supersonic velocities above the wake of the fore component. However, the flow below the wake may be substantially supersonic without the onset of separation.

Lower surface.- The magnitude of the camber and incidence incorporated in the lower surface of the aft component is obviously limited by the required thickness of this component.

Substantial positive camber must be incorporated in the forward region of the aft component to prevent a local negative pressure peak on the upper surface of this component near the leading edge. Further it is believed that the leading-edge radius of the aft component should be relatively small to reduce the adverse influence of the radius on the pressure recovery on the lower surface of the fore component. However, no systematic results have been obtained to determine the optimum radius. The size shown in figure 2(a) was chosen arbitrarily.

Slot

Width.- For maximum effectiveness of the slot flow, the slot exit should be sufficiently wide so that stream energy air is present under the fore component wake along the entire length of the upper surface of the aft component. However, excessive width requires an unnecessarily long slot to provide the desired normal pressure gradient in the slot. (See section on "Curvature.") The width of the slot utilized in the airfoil of figure 2(a) was selected so that the wake of the fore component and the boundary layer of the aft component merge at approximately the trailing edge of the configuration. This width is roughly twice that of the fore-component lower-surface boundary-layer thickness at the exit of the slot. Only the width shown was investigated during the preliminary investigations of this program. However, moderate variations of the width from that shown should have little influence on the effectiveness of the slot.

For the high subsonic Mach numbers under consideration, the flow is choked at the exit of the slot. Further, to minimize the pressure rise on the lower surface of the fore component ahead of the slot, the mean velocity of the flow entering the slot should be substantially greater than the stream value, and, ideally, the entering flow at this point should approach a choked condition. It follows that the slot width at the entrance should very closely approach that at the exit. For the configuration shown in figure 2(a), the area variation was 6 percent. Results from previous phases of the investigation indicate that changes of this variation to 4 and 8 percent had little effect on the effectiveness of the slot. To assure that the flow chokes at the exit rather than at an intermediate point with resulting adverse effects on the operation of the slot, the variation of slot width with length must be carefully controlled with corrections applied for the growth of the boundary layer on both surfaces of the slot.

Curvature.- To reduce the added skin-friction losses of the slot to a minimum, the slot should obviously be as short as possible. Since the length of the slot is primarily an inverse function of its curvature, the curvature should be as severe as possible. However, increasing this curvature exaggerates the velocity gradient across the slot with a resulting adverse increase of Mach number on the lower surface of the slot and an undesirable decrease of Mach number on the upper surface. The curvature obviously must be a compromise. The exploratory experiments indicate that the curvature chosen provides a reasonable velocity gradient across the slot.

To allow changes in the incidence of the aft component with minimum changes of the longitudinal variation of slot area, during the experimental development, the major part of the upper surface of the slot has been made a circular arc with the pivot for changing the incidence of the aft component near the center of this arc. Such a construction might also be advantageous on an actual wing in flight. The use of this circular-arc shape also simplified construction. The desired velocity distribution through the slot has been achieved by properly shaping the lower surface of the slot.

The abrupt reduction of curvature of the stream tube from the slot in the region rearward of the slot (fig. 2(a)) could lead to strong adverse pressure gradients, possibly shock waves, in the flow. To reduce the possibility of such effects, the curvature of the slot has been reduced near the exit over a region extending roughly 1 percent of the airfoil chord forward of the slot exit.

To reduce base drag, the trailing edge of the fore component at the slot exit has been made relatively thin, approximately 0.0006c. Because of the required reduced curvature of the slot upper surface in this region, as described previously, the fore component is thin over an appreciable distance forward of the slot exit. However, the minimum ratio of the local thickness to the length measured forward from the exit is about 0.08, a value which should be structurally feasible.

Selection of Design Conditions

An airfoil-thickness ratio of 0.135 was selected for the model used in the experimental development of the supercritical airfoil. This ratio is somewhat greater than that presently utilized on subsonic aircraft intended to fly near the drag rise. The delay in drag rise provided by the proposed approach should allow the use of larger thickness ratios, which, of course, will provide for either increased aspect ratio or reduction in structural weight.

The airfoil described herein has been designed for a lift coefficient of approximately 0.65. This value is substantially higher than the cruise lift coefficient of most high-subsonic-speed aircraft. The higher value was selected in anticipation that the airfoil would be used on sweptback wings. It is a well-known fact that the effective section of such wings is perpendicular to the swept spanwise elements of the wing. The effective dynamic pressure, acting on these airfoils, is less than the stream value by a function of the square of the cosine of the sweep angle. Therefore, the sections for such wings must be designed for a lift coefficient increased by this ratio. Further, the increased aspect ratio that this concept may allow will require higher lift coefficients for maximum lift-to-drag ratios.

It should be emphasized that the shape shown in figure 2(a) is not necessarily the optimum shape for this thickness ratio and lift coefficient but is merely the shape found to be best at this particular point in the development of the concept. Further, substantial modifications of the shape may be required when it is applied to actual aircraft to achieve the most satisfactory overall design.

EXPERIMENTS

Apparatus and Measurements

Wind tunnel.- The investigation was performed in the Langley 8-foot transonic pressure tunnel. This facility is well suited to the investigation of two-dimensional models since it has solid side walls and slots in the upper and lower walls. With such an arrangement, the side walls act as end plates for a two-dimensional model while the slots allow a development of the flow field in the vertical direction approaching that for free air (ref. 2). For the present research, the opening of the slots was increased from that normally used for transonic testing to reduce the energy losses associated with the induced flow through the slots. The opening at the position of the model was approximately 15 percent of the upper and lower surface walls. The normal opening is about 5 percent.

Models.- Two models, which completely spanned the width of the tunnel (figs. 3 and 4), were investigated: one incorporated the 13.5-percent-thick supercritical airfoil shape; the other, intended to provide a base of reference, embodied an NACA 64_2A215 airfoil section. The shapes of these airfoils are shown in figure 2. Ordinates are presented in tables I to IV. The results presented herein for the supercritical airfoil for angles of attack of 0° and 1° were obtained with the shape for which the ordinates are presented in tables I, II, and III. However, for the results presented for -1° and 3°, the shape differed slightly from that given by the ordinates. Both models were originally constructed with a chord of 18 inches (45.72 cm); however, as a result of modifications, the supercritical airfoil for which results are presented herein has a chord of 19.9 inches (50.55 cm). A reference chord of 20.0 inches (50.8 cm) has been used in reducing the data presented herein for the supercritical airfoil.

In order to achieve minimum deflections of the models at the center of the tunnel, both models are constructed of steel and attached rigidly to the tunnel walls. The plates extending beyond the airfoil lower surface at the wind-tunnel wall, as shown in figures 3 and 4, are a required part of the model attachment. It is believed that the disturbances produced by these protuberances had little influence on the measurements made at the tunnel center line. The angle of attack of the model was changed manually by rotating the model about the pivots shown in figure 3. Both models were investigated in an inverted position.

For the supercritical airfoil, the aft component is attached to the fore component by a series of six strut combinations, as shown in figure 3. These arrangements allow vertical or longitudinal movement and changes of the angle of incidence of the aft component with respect to the fore component. The pivot about which the angle of incidence is changed was located at the approximate center of the curvature of the surface of the slot. The struts attached to the fore component of the airfoil are streamline in shape to reduce the interference of the struts with the boundary layer on the fore component. Other parts of this arrangement were designed for simplicity rather than aerodynamic cleanness. The long vertical extensions of the struts attached to the

fore component as shown in figures 3 and 4 fulfill no function for the tests described herein but are required parts of the supports for nacelles used in an investigation of airfoil-nacelle interference.

The results presented herein for the supercritical airfoil at angles of attack of 0° and 1° were obtained with transition strips of No. 150 carborundum placed on the upper and lower surface of the fore component at 8 percent of the total chord from the leading edge. However, for several reasons, the transition size and location used during earlier phases of the investigation differed from these conditions. On the configuration for which results are presented herein for angles of attack of -1° and 3°, strips of No. 100 carborundum were placed at the 8-percent chord station on the upper surface and at the 40-percent-chord station on the lower surface. On the NACA 64_2A215, strips of No. 100 carborundum were placed at the 40-percent-chord station on both surfaces. The results have been adjusted for these differences by the procedures described in the section entitled "Adjustment of Results." The flow visualizations clearly indicate transition at the strips for all test conditions.

Surface pressure measurements.- The lift and pitching-moment forces acting on the airfoils were obtained from surface pressure measurements. For the supercritical airfoil, surface pressures were measured with orifices located in two chordwise rows at spanwise stations 0.075c and 0.425c from the center line of the tunnel. The row 0.425c from the center line was approximately 0.070c from a strut. The chordwise locations of the orifices are presented in table V. As indicated in the table, for the row 0.075c from the center line, the orifices were concentrated along the rearward region of the airfoil, while in the row 0.425c from the center line the orifices were concentrated along the forward part of the airfoil. The second row of orifices 0.425c from the center line, as well as this special distribution, were required for the investigation of airfoil-nacelle interference. The second row of orifices also provided an indication of the interference of the struts on the flow about the airfoil. The chordwise location of the orifices on the NACA 64_2A215 airfoil are given in table VI.

Pressures were measured with the use of two electronically actuated pressure-scanning-valve units placed in the model near the tunnel walls. The maximum range of the gages in the valves was ± 10 lb/in.^{2} (68 947 newtons/meter^2). To reduce the interference of the orifices on the surface air flow, the diameter of the orifices was made as small as possible, approximately 0.01 inch (0.025 cm).

Wake measurements.- The drag forces acting on the airfoils were derived from vertical variations of the wake total and static pressures measured with the rake shown in figures 3 and 4. The measurement station of the rake was 18 inches (45.72 cm) rearward of the trailing edge of the airfoil. To reduce any errors in the wake measurements associated with disturbances produced by the surface pressure orifices, the rake was displaced laterally 0.05c from the tunnel center line or 0.125c from the center row of orifices as shown in figure 3. The total-pressure tubes were spaced approximately 0.45 percent of the airfoil chord apart in the region of the wake associated with skin-friction boundary losses. In this area, these tubes were flattened horizontally.

Outside this region, the tube spacing progressively widened. In the region where only shock losses were expected, the total-pressure tubes were approximately 10 percent of the chord apart. The rake extended approximately one chord length above the center of the wake and 1/3 chord below. The static pressure tubes were distributed as shown in figure 3. The rake was attached to the conventional sting mount of the Langley 8-foot transonic pressure tunnel. During the investigation, the rake was moved vertically to center the close concentration of tubes on the boundary-layer wake.

The total-head and static pressures were measured with the use of electronically actuated pressure scanning valves. The maximum range of the gage in the valve connected to total-head tubes intended to measure losses in the boundary-layer wake was 5 lb/in.^{2} (34 474 newtons/meter^2); the corresponding range for measuring shock losses was 1 lb/in.^{2} (6894 newtons/meter^2), while that for the static pressures was 1 lb/in.^{2} (6895 newtons/meter^2).

Flow visualization.- Schlieren observations were made with the standard 8-foot transonic pressure tunnel schlieren equipment. Because of the requirement of attaching the model to the steel tunnel structure, schlieren observations could be made only about the rearward part of the airfoils as shown in figure 3. The knife edges of the system were vertical for all of the schlieren photographs presented herein. The vertical broken line on the schlieren photographs is a strip of tape attached to the outer surface of the wind-tunnel wall window. It provides an obvious indication of the longitudinal location of the slot exit. Ahead of the slot exit, the upper surface of the fore component of the model is fairly closely defined by the blackout region; however, downstream of the slot exit the blackout region merely results from a thin end fairing above the aft component.

Surface boundary-layer flow was visualized by the fluorescent oil-film technique described in reference 3. These observations were made for an approximately 5-inch (12.7-cm) wide region centered approximately 12 inches (30.48 cm) from the center line of the tunnel. The protuberances observed in the oil-flow photographs of the upper surface of the airfoil are tubes extending from the trailing edge of the fore component which were used to measure the total- and static-pressure variations in the fore component wake during a preliminary phase of the investigation. These earlier measurements indicated no tendency toward flow reversal in this region and no measurements were made with these tubes thereafter.

Reduction of Data and Accuracy

Pressure measurements.- The section normal-force and section pitching-moment coefficients were first obtained by adding by machine the local pressure coefficients measured at each orifice multiplied by an appropriate weighting factor. Checks of the accuracy of this method for the supercritical airfoil by hand integrations of faired plots of the chordwise pressure variations indicated that this procedure resulted in section normal-force coefficients accurate within 1 percent. Therefore all the normal forces presented herein are based on the machine summation. However, the same checks indicated that the

section pitching-moment coefficients obtained by machine summation were in error by as much as 7 percent primarily because of insufficient number of measurement points near the trailing edge of the airfoil. Therefore, all results for the supercritical airfoil at the more important 0° and 1° angles of attack presented herein were determined by hand integration. The check further indicated that the error was little influenced by angle of attack. Therefore the results obtained by machine for -1° and 3° have been corrected by using the error increments determined for 0° and 1°. All results presented for the NACA 64_2A215 airfoil were obtained by machine summation.

Wake measurements.- To obtain section drag coefficients from the total and static pressures behind the model, point drag coefficients for each of the total-pressure measurements have been computed by using the procedure of reference 4. These point values have then been summed by machine using appropriate weighting factors. Because of the special spacing of the total-pressure tubes, the errors of the results obtained by this procedure are estimated to be less than 1 percent.

Adjustments of results.- As noted in the section on "Models," the results presented herein for angles of attack of -1° and 3° were obtained for a slightly different airfoil shape and transition location than those for 0° and 1°. A comparison of the results obtained at 0° and 1° with and without these differences indicates that they had little effect on the normal-force and pitching-moment characteristics. However, these variations had substantial effects on the drag characteristics. As a rough correction, the differences in drag associated with these effects at 0° and 1° have been applied to the data for -1° and 3°.

As noted in the section describing the models, the location of the transition strip for the NACA 64_2A215 airfoil was different than that for the configuration of the supercritical airfoil for which results are presented herein. The drag characteristics for the NACA 64_2A215 airfoil presented herein have been corrected to a condition corresponding to a transition-strip location the same as that on the supercritical airfoil. This adjustment has been based on the increment obtained for the supercritical airfoil with such a similar transition change. The drag level for the NACA 64_2A215 airfoil obtained by this procedure checks almost exactly the value presented for the same airfoil, corrected for compressibility effects and transition-strip drag, as presented in reference 5.

Corrections for wind-tunnel-wall effects.- The major effect of the wind-tunnel wall on the results presented herein is a substantial up flow at the position of the inverted model so that the real aerodynamic angle of attack is significantly less than the geometric angle. The mean value of this up flow at the midchord of the model, in degrees, as determined by the theory of reference 2, is 2.68 times the section normal-force coefficient. For the design section normal-force coefficient of 0.65, this angle deviation is -1.74°. For the present investigation, wherein the lift-drag and pitching-moment characteristics have been obtained by surface pressure and wake measurements, this deviation has little effect on the validity of these results. It merely causes

a change of the geometric angle of attack at which a given set of results are obtained. The angles of attack used in the results presented herein have not been corrected for this up flow.

The theory of reference 6 indicates that the up flow at the inverted model increases gradually from the leading to the trailing edge. For the design lift coefficient of 0.65 at the optimum Mach number of 0.79, the up flow varied from 1.46 at the leading edge to 2.03 at the trailing edge of the airfoil. The corrected streamline with respect to the airfoil at this condition is shown in figure 2(a). Since the curvature of this induced streamline is quite small compared with those of the various surfaces of the airfoils, it probably has only secondary effects on the characteristics of the models. No corrections have been applied to the results presented to account for this variation.

The theory of reference 2 indicates that the tunnel-wall-blockage effect is trivial.

RESULTS AND DISCUSSION

Basic Aerodynamic Characteristics

The variation of section drag coefficient c_d, angle of attack α, and section pitching-moment coefficient about the quarter chord c_m with section normal-force coefficient c_n at the various test Mach numbers for the supercritical airfoil and for the NACA 64_2A215 airfoil, used as a base of reference, are presented in figures 5 and 6, respectively. (For the relatively low angles of attack of the supercritical airfoil, c_n is approximately equal to the lift coefficient.) Variations of c_d, α, and c_m with Mach number for c_n values of 0.50, 0.65, and 0.80 for the two airfoil shapes, obtained by cross plotting the results of figures 5 and 6, are presented in figure 7. The values obtained from the cross plots are shown by symbols to indicate in detail the unique variations of the characteristics with Mach number. For the supercritical airfoil, these c_n values correspond quite closely to actual test values at Mach numbers just below the abrupt drag rise. These conditions are $\alpha = -1^\circ$ for a Mach number of 0.78, $\alpha = 0^\circ$ for $M = 0.79$, and $\alpha = 1^\circ$ for $M = 0.77$ for the three c_n values selected. Further, it may be noted that for the supercritical airfoil, the variations with Mach number at a c_n value of 0.65 extend beyond the range of the data of figure 5. The experimental results used for this extension were obtained at a single angle of attack of 0°, for which the c_n value was almost exactly 0.65 at these Mach numbers.

Design Normal-Force Condition

For a c_n value of 0.65, the supercritical airfoil experiences a very shallow drag rise to a Mach number of 0.78 then a dip in the drag to a Mach number of 0.79 with an abrupt drag rise beyond this Mach number. (See fig. 7.) The level of drag at a Mach number of 0.79 is only slightly greater

than that for the essentially subcritical conditions at M = 0.65. The Mach number for abrupt drag rise for the supercritical airfoil is approximately 0.12, or 18 percent, higher than the drag rise Mach number of approximately 0.67 estimated for an NACA 64_2A213.5 airfoil on the basis of the results presented in figure 7 for the NACA 64_2A215 airfoil.

Drag at the optimum Mach number condition.- Indications of the phenomena associated with these drag effects are provided by the pressure distributions and schlieren photographs of figure 8, the surface oil-flow photographs of figure 9, and the wake profiles of figure 10. (The scale and longitudinal locations of the schlieren photographs are compatible with the pressure distributions.)

A study of these data indicates that the near elimination of drag rise at a Mach number of 0.79 results not only from a complete elimination of boundary-layer separation on both the upper and lower surfaces (fig. 9), but also from an essentially complete elimination of the shock wave (figs. 8(e) and 10). The pressure distributions of figure 8(e) also indicate a shock-free recompression of the flow to near sonic conditions at the surface of the fore component just ahead of the slot.

The elimination of separation for this condition, even though substantially supercritical flow exists on both the upper and lower surface, results fundamentally and primarily from the actions of the slot as discussed in the section entitled "Basic Concepts." However, the results of the preliminary experiments indicate that the supporting special shapings of the airfoil as described in the section entitled "Development of Detailed Shape" are required to achieve the final complete elimination of separation shown herein.

The elimination of shock losses was unexpected. The exact nature of the phenomena leading to this effect is not yet fully understood. However, the fact that a similar shock-free recompression occurs in the same region of the airfoil for a Mach number of 0.78, for which condition the flow field ahead of this region is substantially different, suggests that the effect is not achieved by a special, longitudinal distribution of the decelerating disturbances, described in reference 1, which originate at the outer boundary of the forward supersonic region.

An analysis of the surface pressure measurements and schlieren photographs suggests rather that this shock-free recompression is accomplished by a controlled, forward movement of decelerating disturbances associated with the pressure recovery near the trailing edge of the airfoil. The Mach number at the airfoil surface just rearward of this region of shock-free recompression is slightly supersonic. (See fig. 8(e).) Therefore, the aft-originating positive disturbances cannot move forward near the surface to converge into the usual shock wave. However, the schlieren photograph of figure 8(e) indicates that the flow in this same longitudinal region at a moderate distance above the airfoil surface (about 0.3 chord) is subsonic so that these disturbances can move forward above the local supersonic region near the surface. These disturbances can then move downward into the supersonic region to decelerate the flow essentially shock free. Results obtained for other slightly different configurations

indicate that the most important element in obtaining shock-free recompression is the presence of the slightly supersonic flow just ahead of the slot. When the Mach number in this region is subsonic, shock-free recompression is not achieved. For such a condition, the aft-originating disturbances move directly forward near the surface to form a shock wave in the usual manner.

The flow on the upper surface of the aft component outside the slot reaches a maximum Mach number of approximately 1.1, corresponding to a pressure coefficient of 0.68, but no indication of a shock wave on this surface is present. The apparent elimination of the shock in this region is believed to be due to factors similar to those that cause the same effect above the fore component but with the actions exaggerated by the presence of the low-energy wake of the fore component above this surface.

The drag level at the optimum Mach number is approximately 10 percent greater than that for the NACA 64_2A215 at Mach numbers below the drag rise. (See fig. 7(a).) This increment is due primarily to differences in the skin-friction losses for the two configurations; the additional loss is associated with the added wetted area of the slot as well as with the lower Reynolds number for the boundary-layer flow on the aft component compared with that for the corresponding region on the reference airfoil.

Drag at Mach numbers below the optimum value.- The surface oil-flow photographs (fig. 9) indicate no boundary-layer separation on either the upper or lower surface at any Mach number below the optimum value. The gradual drag rise at Mach numbers to roughly 0.78 is associated with wave losses (fig. 10) in the weak shock wave present above the middle region of the upper surface of the fore component (fig. 8).

Drag rise above the optimum Mach number.- The abrupt drag rise at Mach numbers above 0.79 is caused by increased wave losses (fig. 10) and boundary-layer separation on the upper surface of the aft component associated with a shock just rearward of the slot exit (fig. 8(g)).

The surface oil-film photographs of figure 9 indicate no significant separation on the lower surface of the fore component for Mach numbers to 0.80 in spite of a substantial increase in the strength of the shock-wave pressure rise below that surface (fig. 8(g)).

Results obtained for earlier configurations indicate that, when the Mach number is increased beyond 0.80 for this value of c_n, the boundary layer on the lower surface of the fore component finally separates with a resulting substantial loss of normal force. The usefulness of further refinements of the shape of the upper surface of the supercritical airfoil to provide an additional delay of the abrupt drag rise, associated with the movement of the shock rearward of the slot, is primarily dependent on the achievement of a delay of this lower-surface separation to a higher Mach number. The subcritical pressure distribution on the lower surface of the fore component (fig. 8(b)) incorporates the long region of nearly constant velocity discussed in the section entitled "Development of Detailed Shape." A further reduction in strength of the shock on the lower surface might be accomplished by shaping this surface to provide

a saddle-back subcritical pressure distribution similar to that achieved for the upper surface (fig. 8(a)) with a reduced induced pressure near the crest line for this surface. Also, the measured pressure rise ahead of the slot is greater than that indicated as most desirable in the section on "Development of Detailed Shape." Reshaping this surface to provide the desired rise would be expected to delay the onset of separation.

Pitching moment at optimum Mach number.- At the optimum Mach number for the supercritical airfoil, $M = 0.79$, the section pitching-moment coefficient for this shape is approximately -0.20 compared with a value of approximately -0.05 for the NACA 64_2A215 at Mach numbers below the drag rise. (See fig. 7(c).) This very large increase in c_m is associated primarily with the substantial load carried by the aft component. Integration of the pressure distributions indicates that at this Mach number the normal force on the aft component is 0.4 of the total. This large pitching moment is inherent in the design of the supercritical airfoil shape.

Off-Design Normal-Force Conditions

Normal force above design value.- At a c_n value of 0.8, the supercritical airfoil experiences the same dip in the variation of c_d with Mach number as obtained at the design c_n value of 0.65. (See fig. 7(a).) In this case, the drag dip occurs at a Mach number of approximately 0.77. Wake profiles, not presented, indicate that, as for the design normal-force condition, this dip is associated with a substantial reduction in the shock loss. The pressure distributions presented in figure 11 indicate a gradual, apparently shock-free pressure recovery on the upper surface in a region somewhat forward of that for which the same recovery occurred at the design condition. Because of the limited field of observation of the schlieren system described in the section on "Apparatus and Measurements," schlieren photographs could not be obtained in the vicinity of this pressure recovery to elucidate the nature of the flow field for this region. It may be noted that the surface Mach number rearward of this region of apparently shock-free recompression is slightly supersonic (fig. 11) as at the design normal-force condition.

The additional normal force associated with increased angle of attack is centered near the quarter-chord point of the airfoil at all Mach numbers to 0.77. (See figs. 5(c) and 7(c).)

High normal force.- For an angle of attack of 3°, the highest test value, the c_n values at Mach numbers of 0.65, 0.70, and 0.75 are 1.24, 1.02, and 1.14, respectively. (See fig. 5.) In spite of large abrupt adverse pressure gradients on the upper surface of the fore component, due to the presence of a very strong shock wave (fig. 12), the surface oil flows presented in figure 13 indicate that no significant separation occurs on the upper surface for these conditions. The wake profiles (not presented) indicate that most of the increase in drag associated with increasing the angle of attack to these values is due to greatly magnified shock losses. Further, the results presented in figure 5(b) indicate that the slope of the variation of c_n with α increases

as α is increased to 3°. The decrease in c_n at $M = 0.70$ compared with the values obtained at the lower and higher Mach numbers results from a marked forward movement of the shock wave for this condition. (See fig. 12.) The phenomenon associated with this deviation is not understood.

In contrast to these characteristics noted for the supercritical airfoil, the reference NACA 64_2A215 airfoil experiences a substantial decrease in the variation of c_n with α at c_n values greater than approximately 0.95 for Mach numbers of 0.65 and 0.67 and at substantially lower c_n values for the higher Mach numbers. (See fig. 6(b).) Thus it is apparent that the shape of the supercritical airfoil, particularly the slot, substantially improves the high-lift stall characteristics for high Mach numbers, at least.

Normal force below design value.- The variation of c_d with Mach number for the supercritical airfoil at c_n of 0.5 indicates a drag rise at a Mach number of 0.79 (fig. 7(a)). The wake profiles (not presented) indicate that this drag rise is due, in roughly equal increments, to the onset of shock-induced separation on the lower surface of the airfoil and to shock losses above the airfoil. The pressure distributions of figure 14 indicate that these losses result from the presence of substantial regions of supersonic velocities on the lower surface of the fore component and on the aft region of the upper surface. Obviously, the operation of the supercritical airfoil is critical at c_n values below the design value.

An analysis of the pressure distributions of figure 14 suggests that the onset of the several adverse effects at this lower off-design normal force could probably be delayed by reducing the relative angle of the aft component and recovering the resulting lift loss by a somewhat higher angle of attack. Such a change on an actual aircraft would, of course, require providing means for varying the incidence of the aft component in cruise flight.

CONCLUSIONS

A wind-tunnel investigation has been made at Mach numbers from 0.65 to 0.80 of two-dimensional models of two 13.5-percent-thick airfoils. One, a supercritical airfoil, is intended to delay drag rise beyond the critical Mach number; the other, an NACA 64A-series section, provides a basis of comparison. Results of this investigation indicate the following:

1. For a section lift coefficient of 0.65, the design value, the abrupt drag rise for the supercritical airfoil occurs at a Mach number just above 0.79. The corresponding drag-rise Mach number for the NACA 64A-series airfoil of the same thickness ratio is 0.67. The drag at a Mach number just less than that for drag rise is due almost entirely to skin-friction losses. The drag value at this condition is approximately 10 percent greater than that for the NACA 64A-series airfoil.

2. The section pitching-moment coefficient for the supercritical airfoil shape is substantially more negative than that for more conventional sections.

3. The supercritical airfoil also provides delays in the drag rise at off-design section lift coefficients.

4. The supercritical airfoil provides a substantial increase in the stall section normal-force coefficients at high subsonic Mach numbers.

5. The operation of the supercritical airfoil appears most critical at section normal-force coefficients below the design value.

Langley Research Center,
National Aeronautics and Space Administration,
Langley Station, Hampton, Va., April 20, 1965.

REFERENCES

1. Pearcey, H. H.: Shock-Induced Separation and Its Prevention by Design and Boundary Layer Control. Boundary Layer and Flow Control, Vol. 2, G. V. Lachmann, ed., Pergamon Press, 1961, pp. 1166-1344.

2. Davis, Don D., Jr.; and Moore, Dewey: Analytical Study of Blockage- and Lift-Interference Corrections for Slotted Tunnels Obtained by the Substitution of an Equivalent Homogeneous Boundary for the Discrete Slots. NACA RM L53E07b, 1953.

3. Loving, Donald L.; and Katzoff, S.: The Fluorescent-Oil Film Method and Other Techniques for Boundary-Layer Flow Visualization. NASA MEMO 3-17-59L, 1959.

4. Baals, Donald D.; and Mourhess, Mary J.: Numerical Evaluation of the Wake-Survey Equations for Subsonic Flow Including the Effect of Energy Addition. NACA WR L-5, 1945. (Formerly NACA ARR L5H27.)

5. Abbott, Ira H.; Von Doenhoff, Albert E.; and Stivers, Louis S., Jr.: Summary of Airfoil Data. NACA Rept. 824, 1945. (Supersedes NACA WR L-560.)

6. Katzoff, S.; and Barger, Raymond L.: Boundary-Induced Downwash Due to Lift in a Two-Dimensional Slotted Wind Tunnel. NASA TR R-25, 1959. (Supersedes NACA TN 4289.)

TABLE I.- ORDINATES FOR SUPERCRITICAL AIRFOIL

[All dimensions in percent chord where c = 20 in. (50.8 cm)]

Fore component			
Upper surface		Lower surface	
x	z	x	z
0	4.725	0	4.725
.25	5.525	.25	4.050
.50	5.875	.50	3.750
.75	6.140	.75	3.450
1.00	6.375	1.00	3.200
2.50	7.350	2.50	2.225
3.75	7.825	3.75	1.550
5.00	8.175	5.00	1.050
7.50	8.675	7.50	.175
10.00	8.975	10.00	-.525
12.50	9.200	12.50	-1.150
15.00	9.375	15.00	-1.675
17.50	9.525	17.50	-2.110
20.00	9.600	20.00	-2.475
25.00	9.775	25.00	-3.000
30.00	9.825	30.00	-3.375
35.00	9.865	35.00	-3.575
40.00	9.865	40.00	-3.610
45.00	9.825	45.00	-3.525
50.00	9.675	50.00	-3.300
52.50	9.575	52.50	-3.125
55.00	9.475	55.00	-2.900
57.50	9.360	57.50	-2.615
60.00	9.225	60.00	-2.250
62.50	9.060	62.50	-1.815
65.00	8.850	65.00	-1.250
67.50	8.650	67.50	-.500
70.00	8.425	70.00	.500
72.50	8.200	72.50	2.100
75.00	7.910	73.75	3.425
77.50	7.650	75.00	4.800
78.75	7.500	76.25	5.750
80.00	7.325	77.50	6.360
81.25	7.175	78.75	6.750
83.00	6.950	80.00	6.940
		81.00	7.040
		82.00	6.975
		83.00	6.900
L.E. radius: 1.500			

Aft component			
Upper surface		Lower surface	
x	z	x	z
75.30	1.875	75.30	1.875
75.50	2.575	75.50	1.865
75.75	2.875	75.75	2.075
76.00	3.140	76.00	2.250
76.25	3.375	76.25	2.385
76.50	3.610	76.50	2.500
77.00	4.000	77.00	2.650
77.50	4.275	77.50	2.750
78.00	4.575	78.00	2.800
78.75	4.860	78.75	2.775
80.00	5.150	80.00	2.700
81.25	5.250	81.25	2.575
82.50	5.175	82.50	2.475
83.75	5.000	83.75	2.375
85.00	4.800	85.00	2.250
86.25	4.575	86.25	2.125
87.50	4.325	87.50	2.000
88.75	4.025	88.75	1.875
90.00	3.750	90.00	1.750
91.25	3.365	91.25	1.550
92.50	2.975	92.50	1.375
93.75	2.500	93.75	1.150
95.00	2.025	95.00	.900
96.25	1.500	96.25	.625
97.50	.950	97.50	.400
98.75	.360	98.75	.150
99.50	0	99.50	0
L.E. radius: 0.150			

TABLE II.- VARIATION IN WIDTH OF SLOT*

[c = 20 in. (50.8 cm)]

Station, percent chord from L.E. of airfoil	Slot width, percent chord
74.0	1.925
74.5	1.860
75.0	1.855
75.5	1.855
76.0	1.845
76.5	1.835
77.0	1.830
77.5	1.815
78.0	1.805
78.5	1.800
79.0	1.800
79.5	1.800
80.0	1.800
80.5	1.795
81.0	1.790
81.5	1.770
82.0	1.755
82.5	1.750
83.0	1.750

*Measurements at the stations are taken perpendicular to the lower surface of the fore component.

TABLE III.- THICKNESS OF THE TRAILING EDGE OF THE FORE COMPONENT

[c = 20 in. (50.8 cm)]

Station, percent chord from L.E. of airfoil	T.E. thickness, percent chord
78.5	0.910
79.0	.705
79.5	.525
80.0	.385
80.5	.260
81.0	.165
81.5	.115
82.0	.080
82.5	.060
83.0	.050

TABLE IV.- ORDINATES FOR NACA 64_2A215 AIRFOIL

[All dimensions in percent chord where c = 18 in. (45.72 cm)]

Upper surface		Lower surface	
x	z	x	z
0	0	0	0
.388	1.243	.612	-1.131
.624	1.509	.876	-1.351
1.107	1.930	1.393	-1.688
2.333	2.713	2.667	-2.291
4.811	3.833	5.189	-3.111
7.304	4.683	7.696	-3.711
9.802	5.391	10.198	-4.199
14.811	6.510	15.189	-4.948
19.827	7.351	20.173	-5.491
24.849	7.975	25.151	-5.873
29.875	8.417	30.125	-6.121
34.903	8.686	35.097	-6.238
39.933	8.766	40.067	-6.208
44.963	8.627	45.037	-5.999
49.992	8.308	50.008	-5.648
55.018	7.843	54.982	-5.191
60.042	7.258	59.958	-4.654
65.063	6.566	64.937	-4.056
70.079	5.782	69.921	-3.416
75.093	4.926	74.907	-2.766
80.111	4.017	79.889	-2.147
85.109	3.039	84.891	-1.597
90.076	2.046	89.924	-1.066
95.039	1.039	94.961	-.549
100.000	.032	100.000	-.032
L.E. radius: 1.561			

TABLE V.- ORIFICE LOCATIONS ON THE SUPERCRITICAL AIRFOIL

[All dimensions in percent chord from L.E. of airfoil where c = 20 in. (50.8 cm)]

Orifice row at 0.075c from airfoil center line	
Upper surface	Lower surface
Fore component	
1.0 5.0 10.5 18.2 28.1 38.9 48.8 56.0 61.4 66.8 72.2 76.7 80.3	5.0 10.2 16.0 23.6 32.6 41.6 47.9 53.3 57.8 61.4 65.0 68.2 70.9 73.6 75.8 77.6 79.4 81.2 82.6
Aft component	
75.5 75.6 75.8 76.1 77.4 79.2 81.0 82.8 84.6 86.9 90.0 93.6	76.1 77.4 80.6 85.1 89.6 95.9

Orifice row at 0.425c from airfoil center line	
Upper surface	Lower surface
Fore component	
1.0 4.0 7.9 11.9 16.4 22.7 29.9 37.1 44.3 50.6 57.8 66.8 75.8 81.7	1.0 4.0 7.9 11.9 16.0 20.9 26.3 31.7 37.1 42.5 47.9 53.3 58.7 64.1 69.5 73.6 76.3 79.0 81.7
Aft component	
76.5 78.8 81.5 84.2 87.3 92.3	76.5 79.2 84.6

TABLE VI.- ORIFICE LOCATIONS ON THE NACA 64_2A215 AIRFOIL

[All dimensions in percent chord from L.E. of airfoil where c = 18 in. (45.72 cm)]

Orifice location on -	
Upper surface	Lower surface
0.5	0.5
2.5	2.5
6.0	6.0
11.0	10.5
18.0	16.0
26.0	22.0
33.0	28.0
38.0	34.0
42.0	40.0
46.0	46.0
50.0	52.0
54.0	58.0
58.5	64.0
64.0	70.0
70.0	76.0
76.0	82.0
82.0	88.0
88.0	94.0
94.0	98.5
98.5	

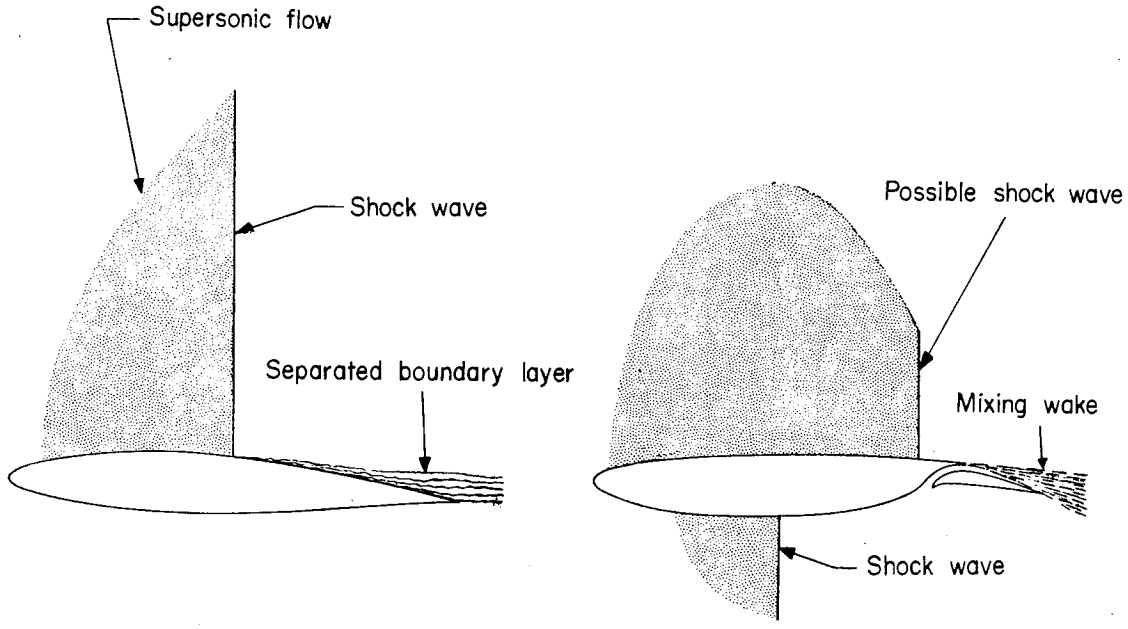

Flow fields

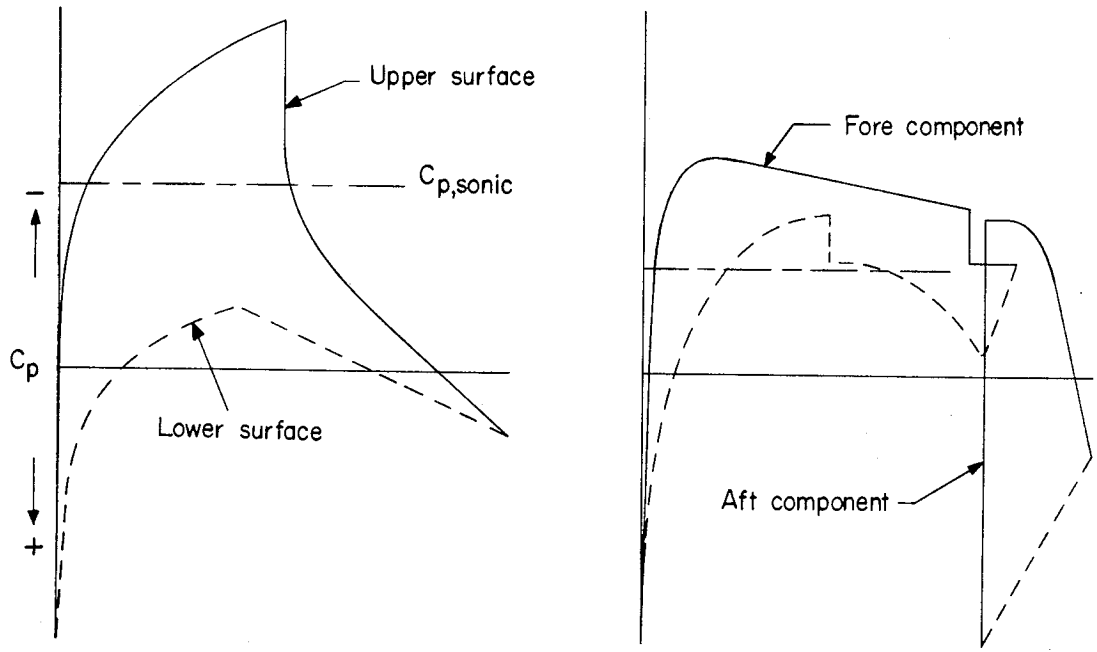

Surface pressure distributions

NACA 64A-series airfoil, M=0.69

Supercritical airfoil, M=0.79

Figure 1.- Schematic illustration of supercritical phenomena at cruise lift conditions.

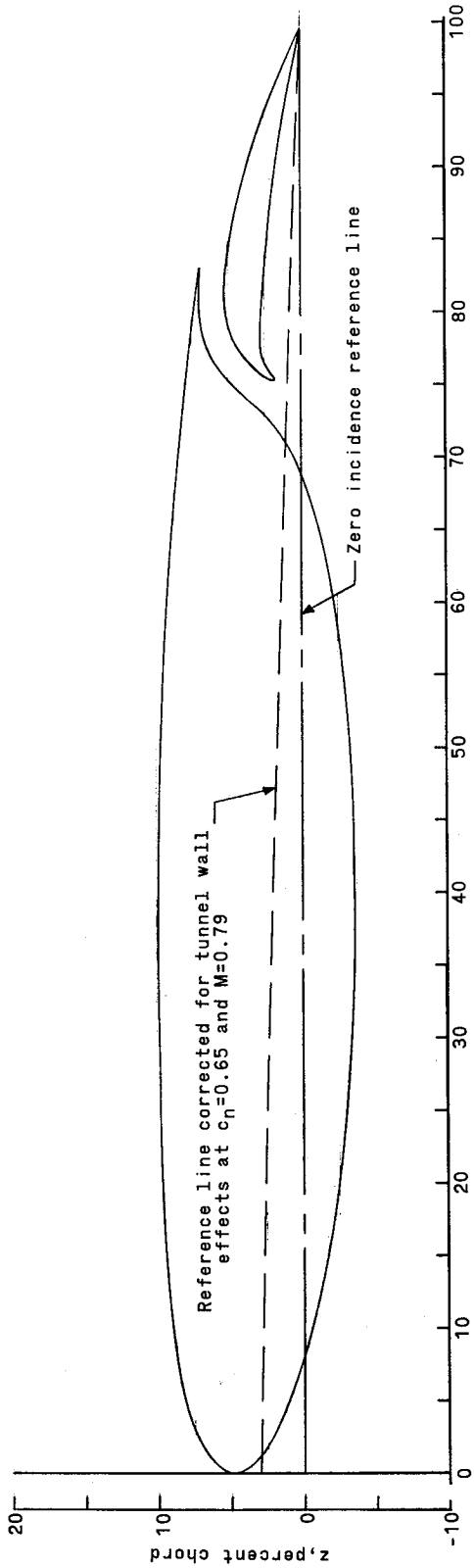

(a) Supercritical airfoil.

Figure 2.- Cross section of test airfoils.

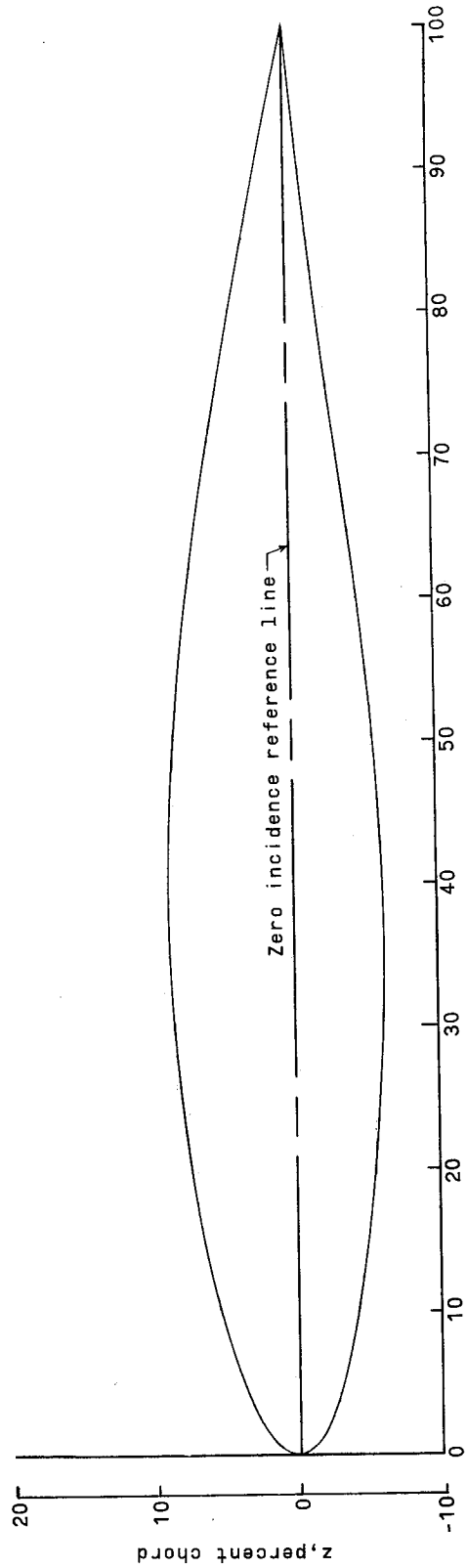

(b) NACA 64_2A215 airfoil.

Figure 2.- Concluded.

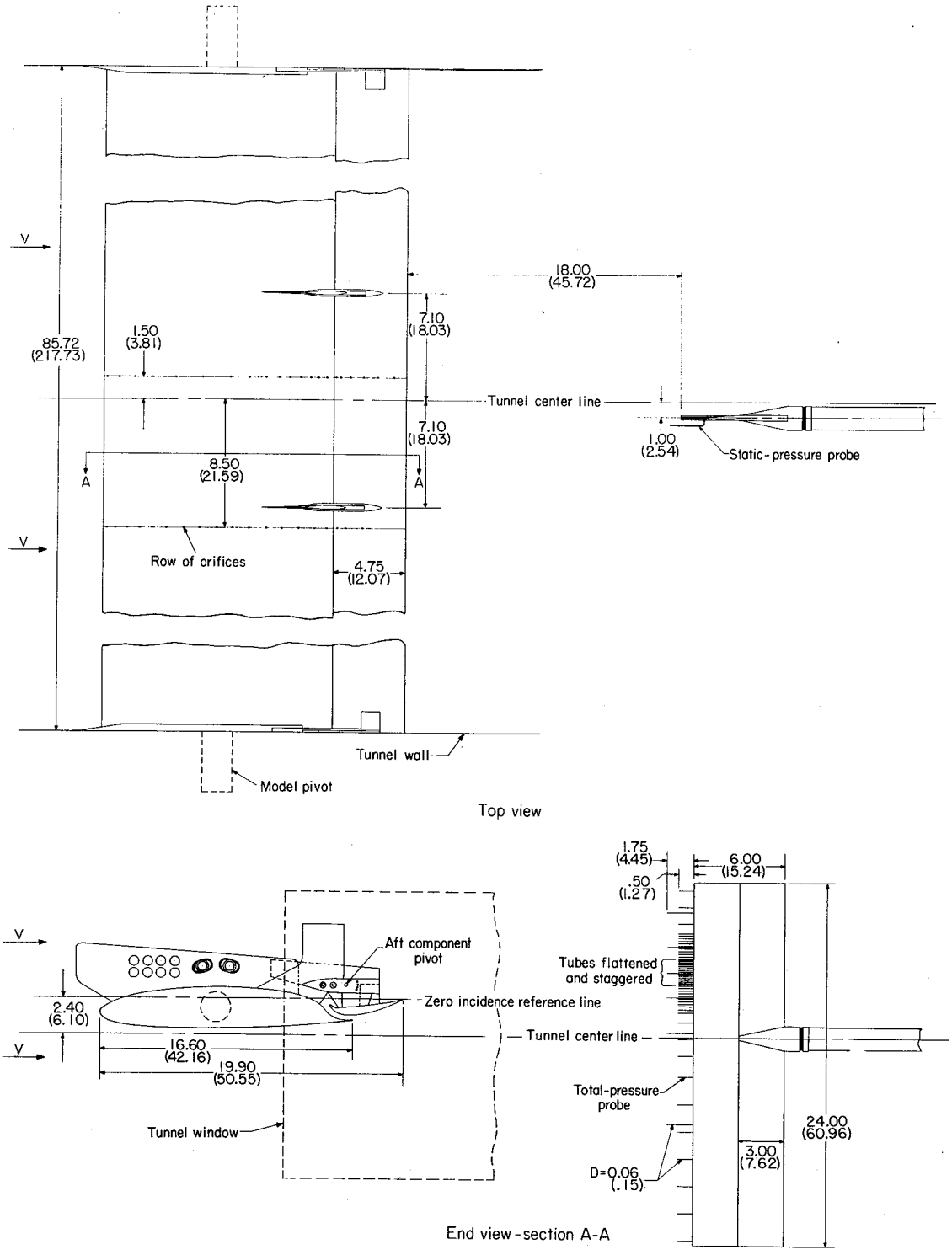

Figure 3.- Two-view drawing of apparatus. (All dimensions are inches (centimeters in parentheses).)

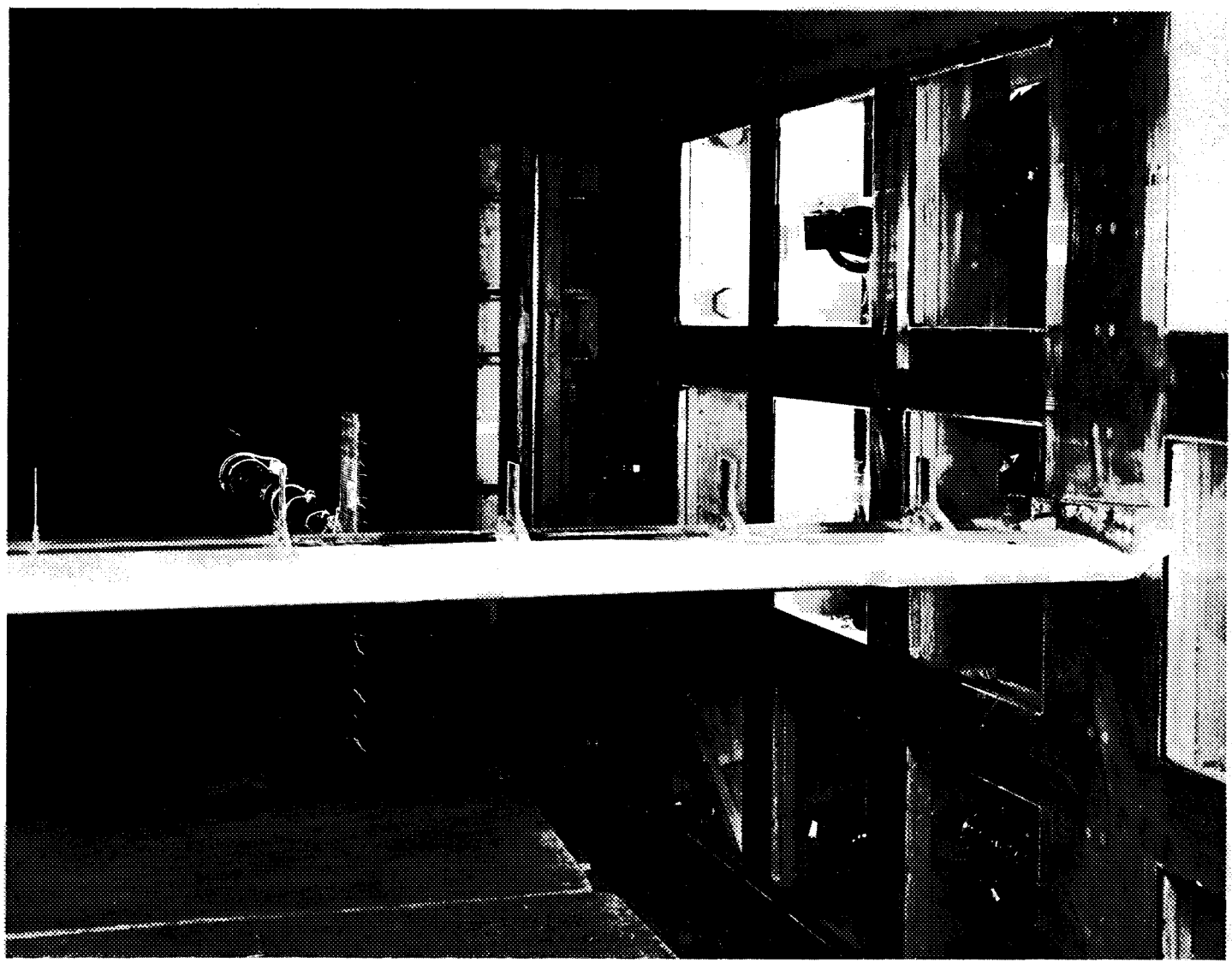

(a) Front view. L-64-8926.1

Figure 4.- Photograph of apparatus.

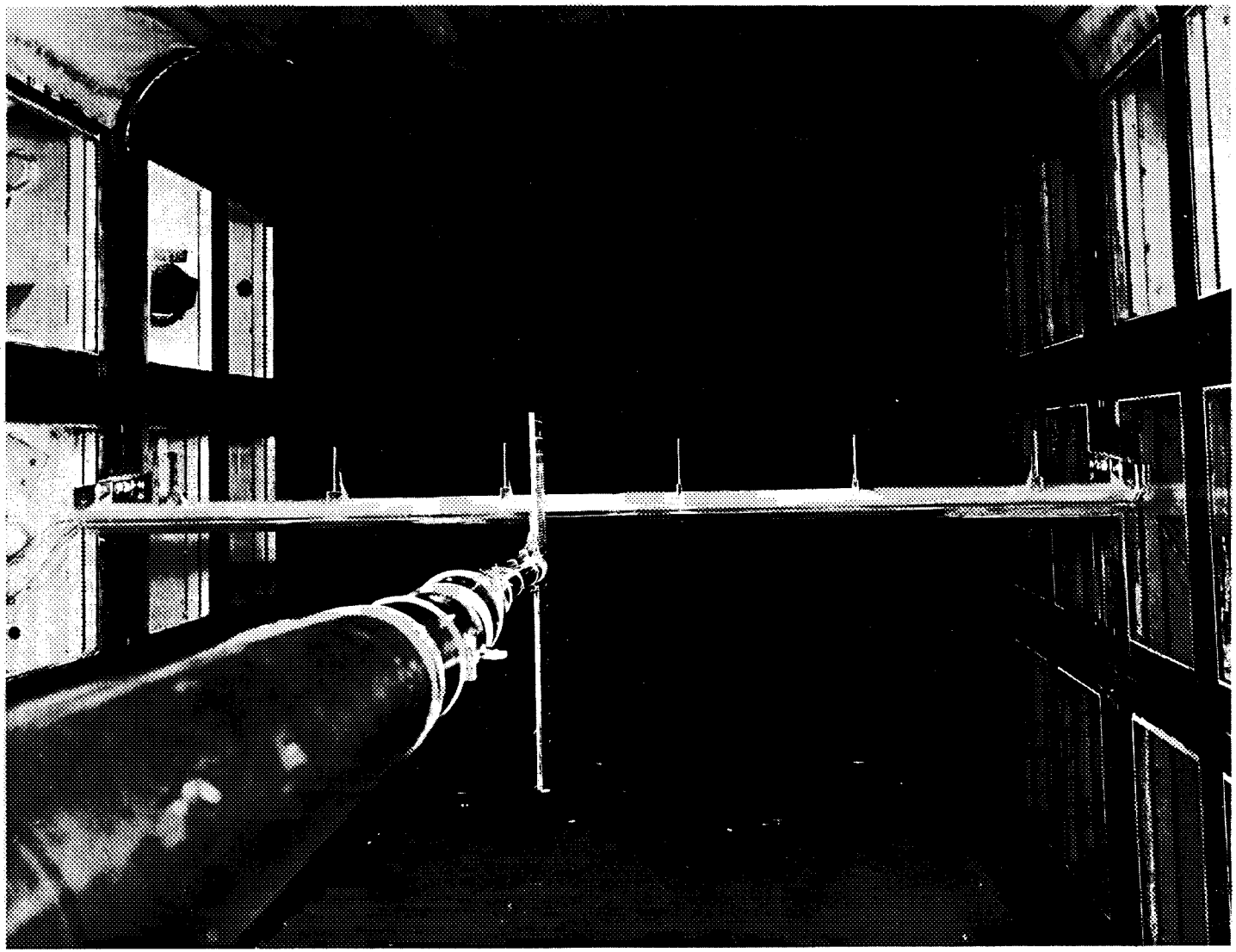

(b) Rear view. L-64-8925

Figure 4.- Concluded.

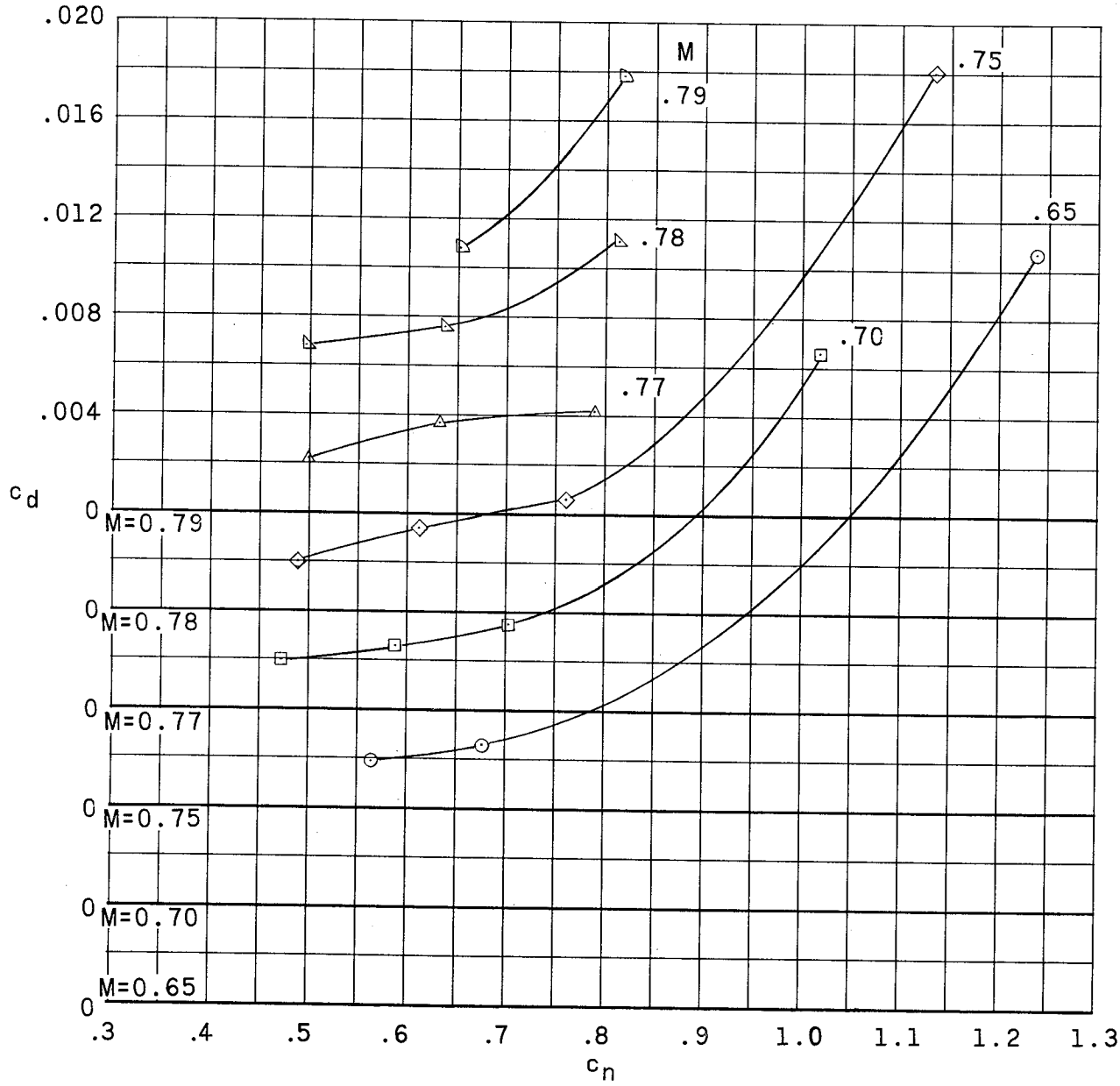

(a) Drag.

Figure 5.- Variation of section drag coefficient, angle of attack, and section pitching-moment coefficient with section normal-force coefficient at various Mach numbers for supercritical airfoil.

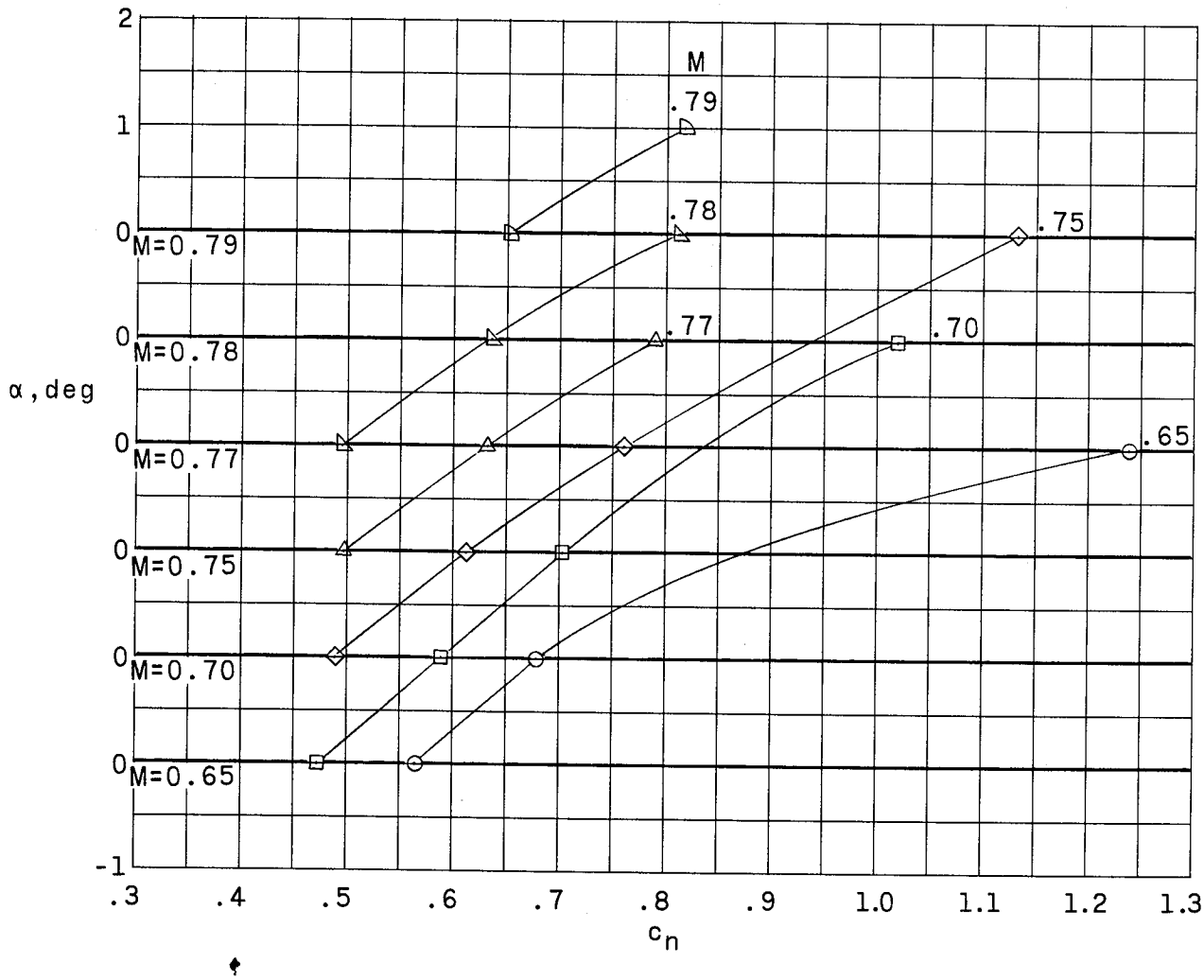

(b) Angle of attack.

Figure 5.- Continued.

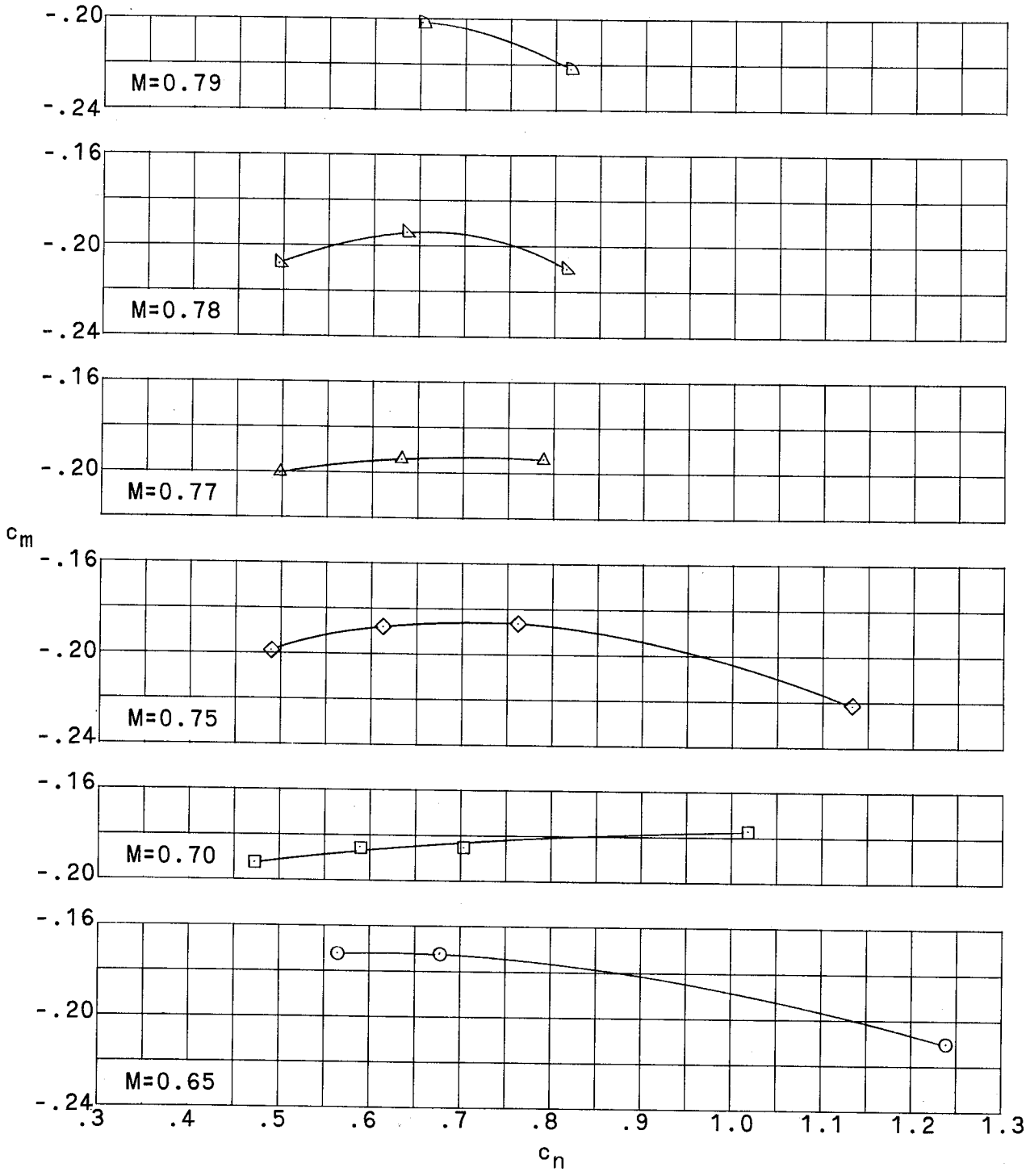

(c) Pitching moment.

Figure 5.- Concluded.

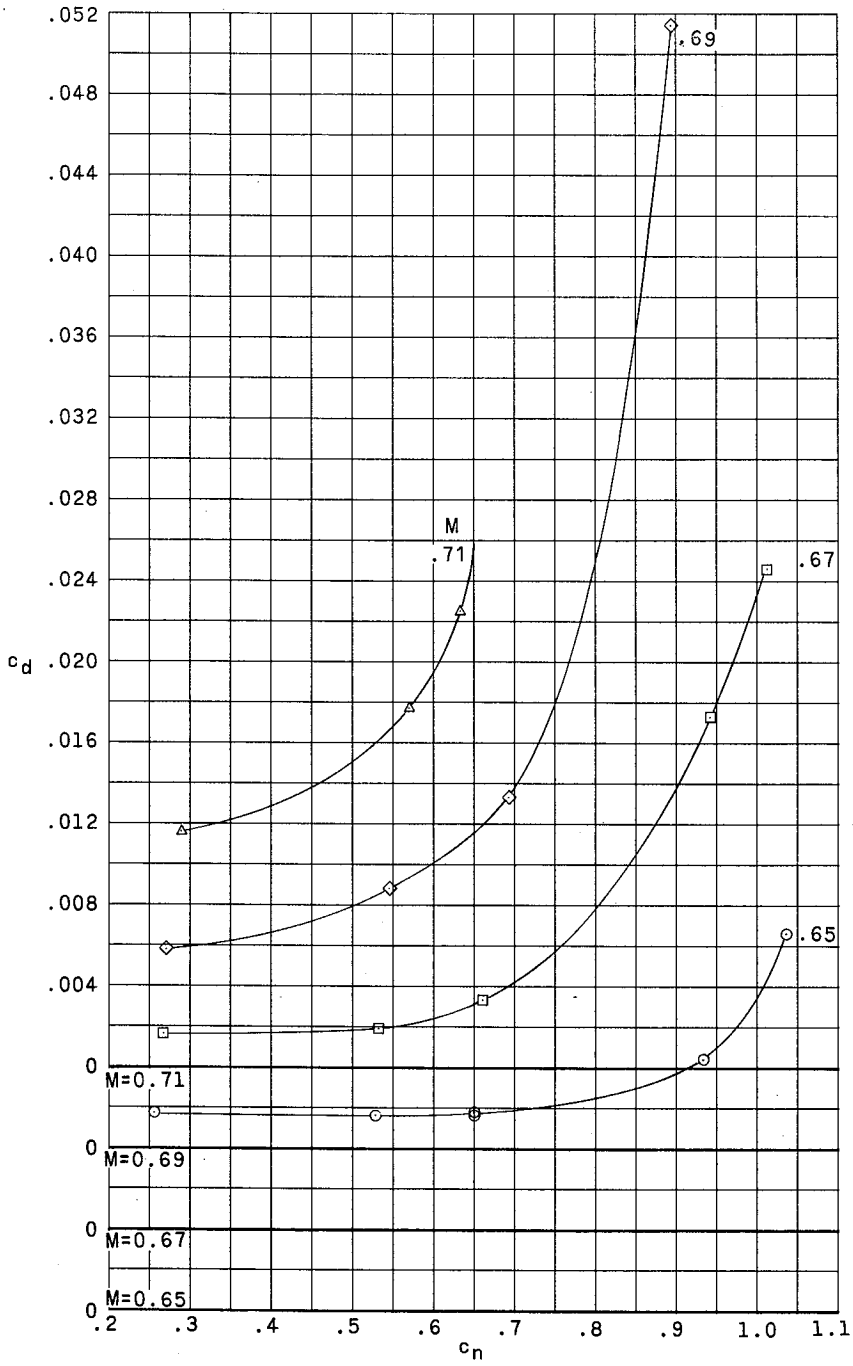

(a) Drag.

Figure 6.- Variation of section drag coefficient, angle of attack, and section pitching-moment coefficient with section normal-force coefficient at various Mach numbers for NACA 64_2A215 airfoil.

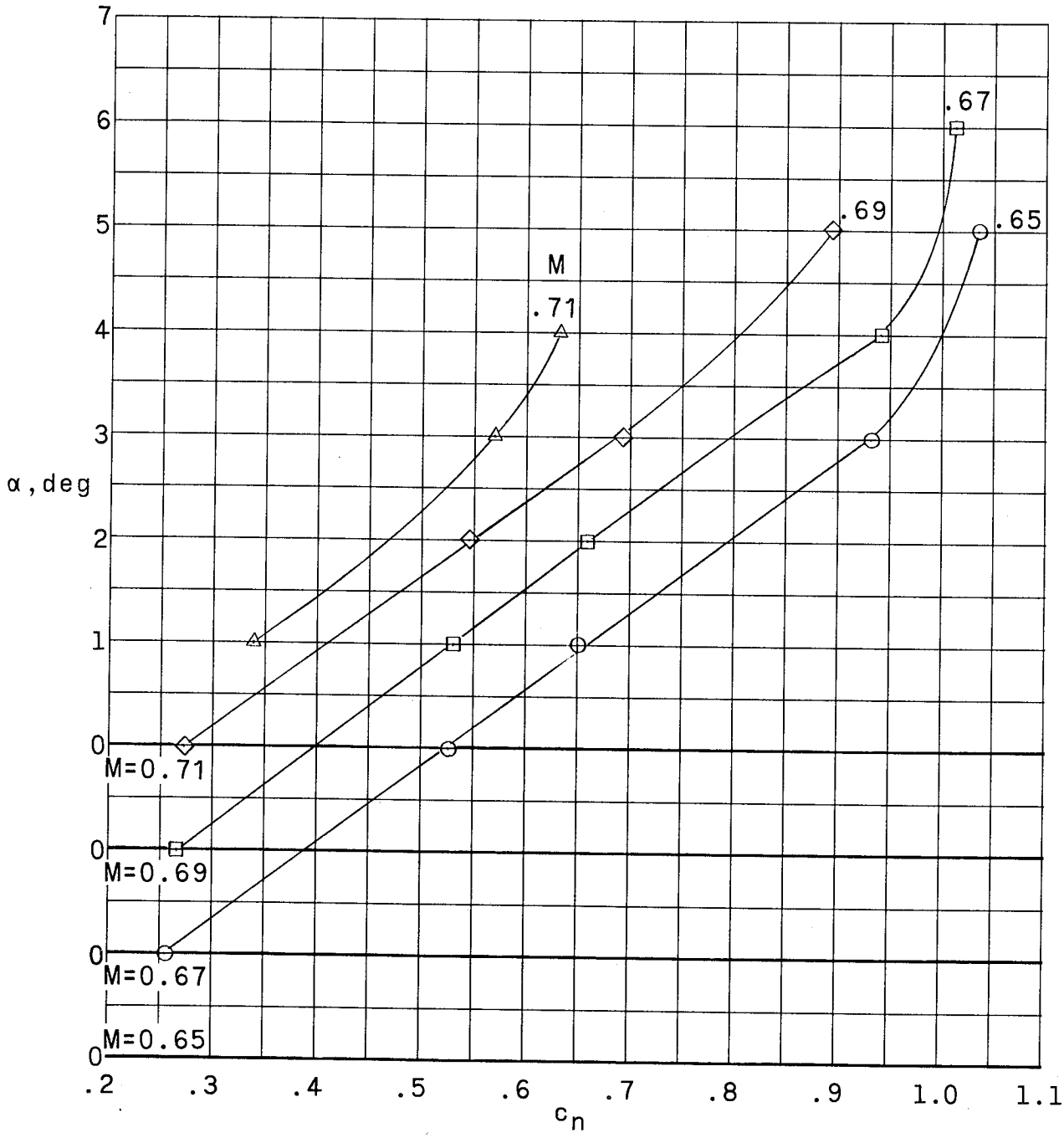

(b) Angle of attack.

Figure 6.- Continued.

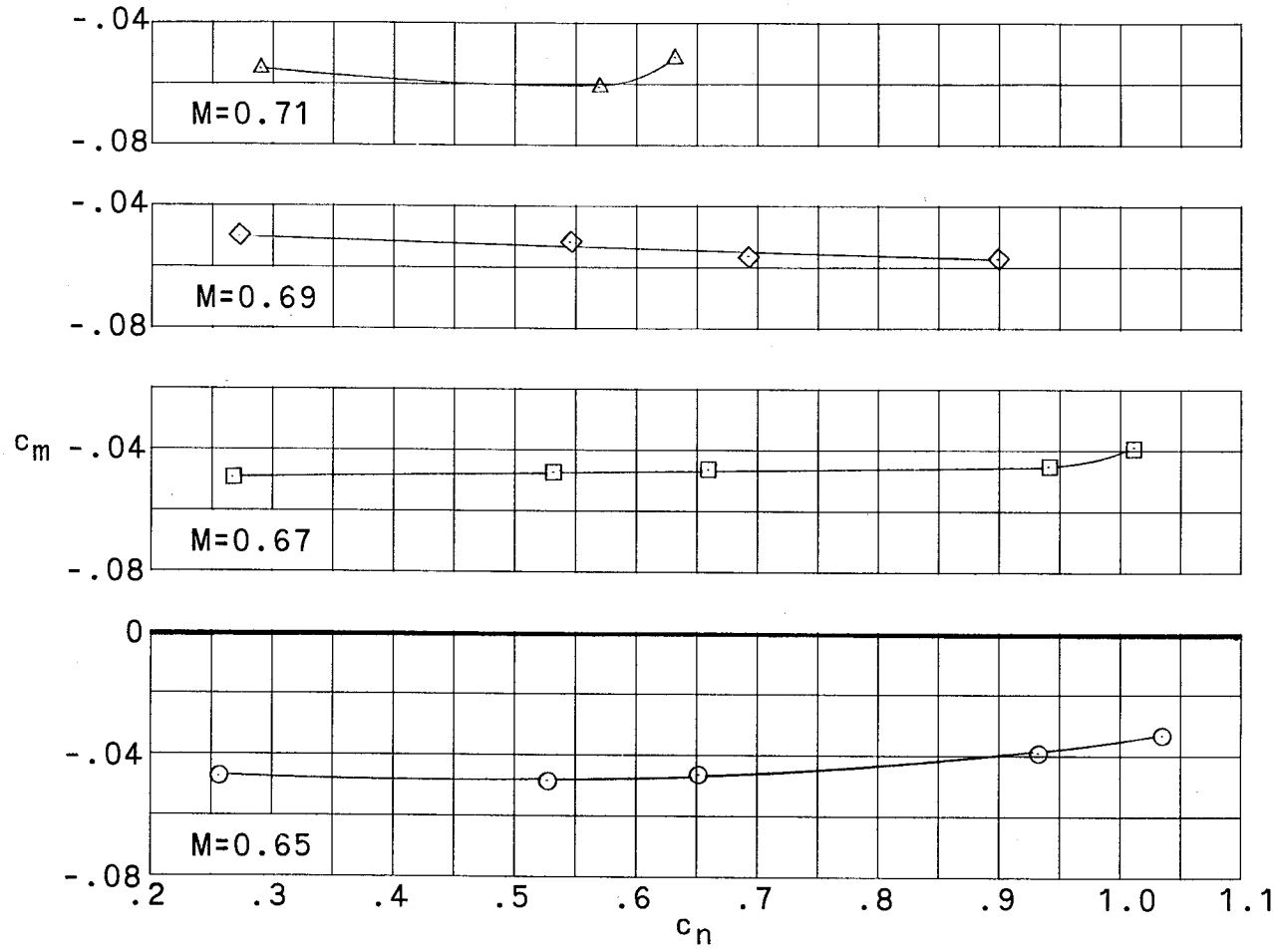

(c) Pitching moment.

Figure 6.- Concluded.

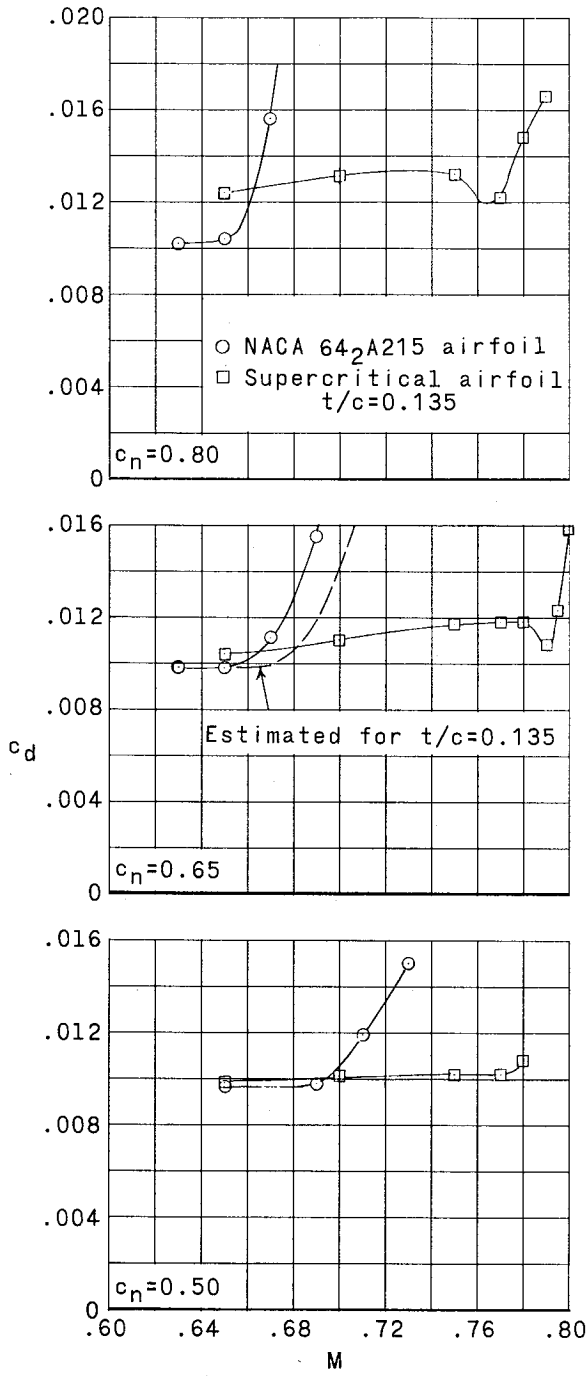

(a) Drag.

Figure 7.- Variation of section drag coefficient, angle of attack, and section pitching-moment coefficient with Mach number for several section normal-force coefficients.

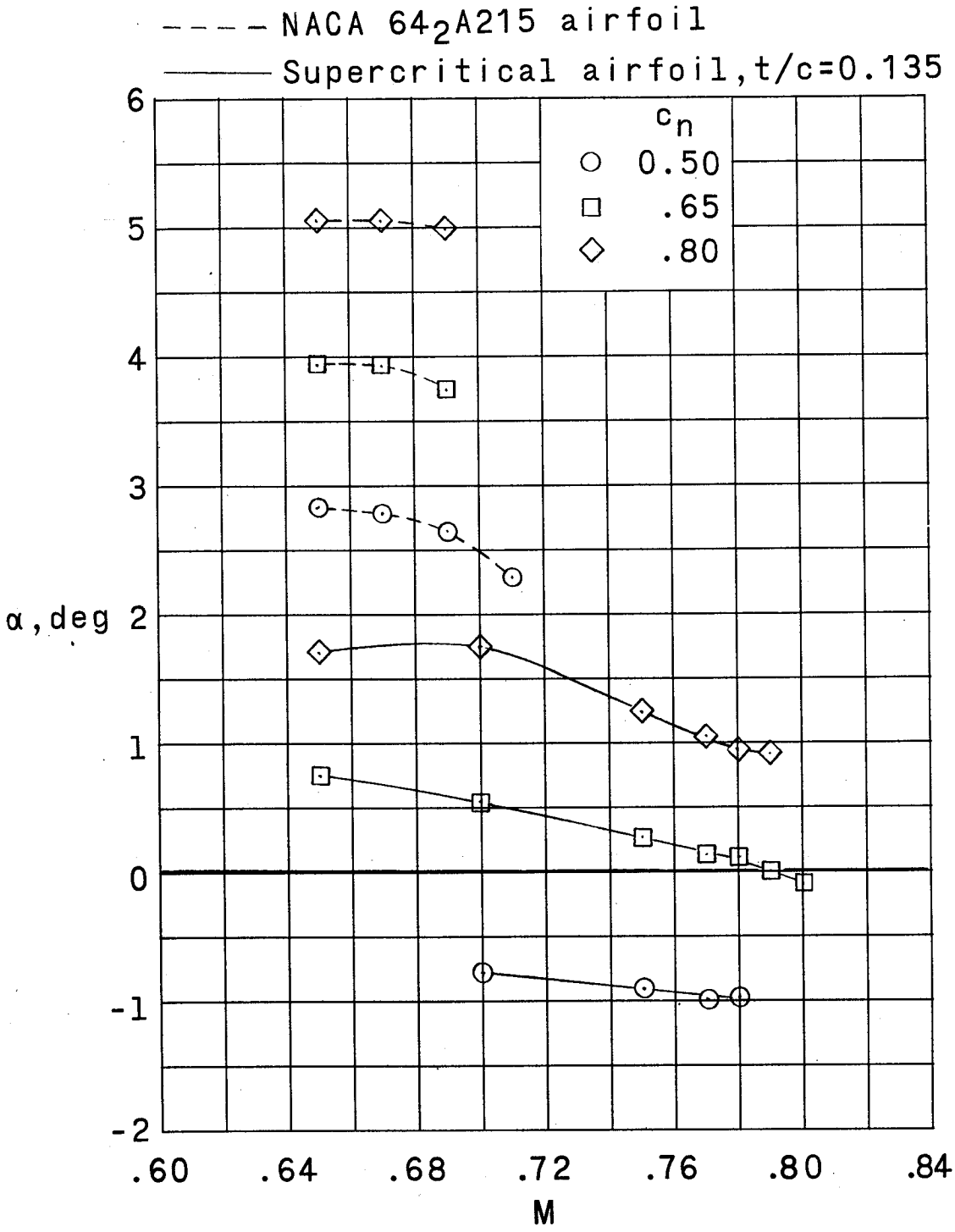

(b) Angle of attack.

Figure 7.- Continued.

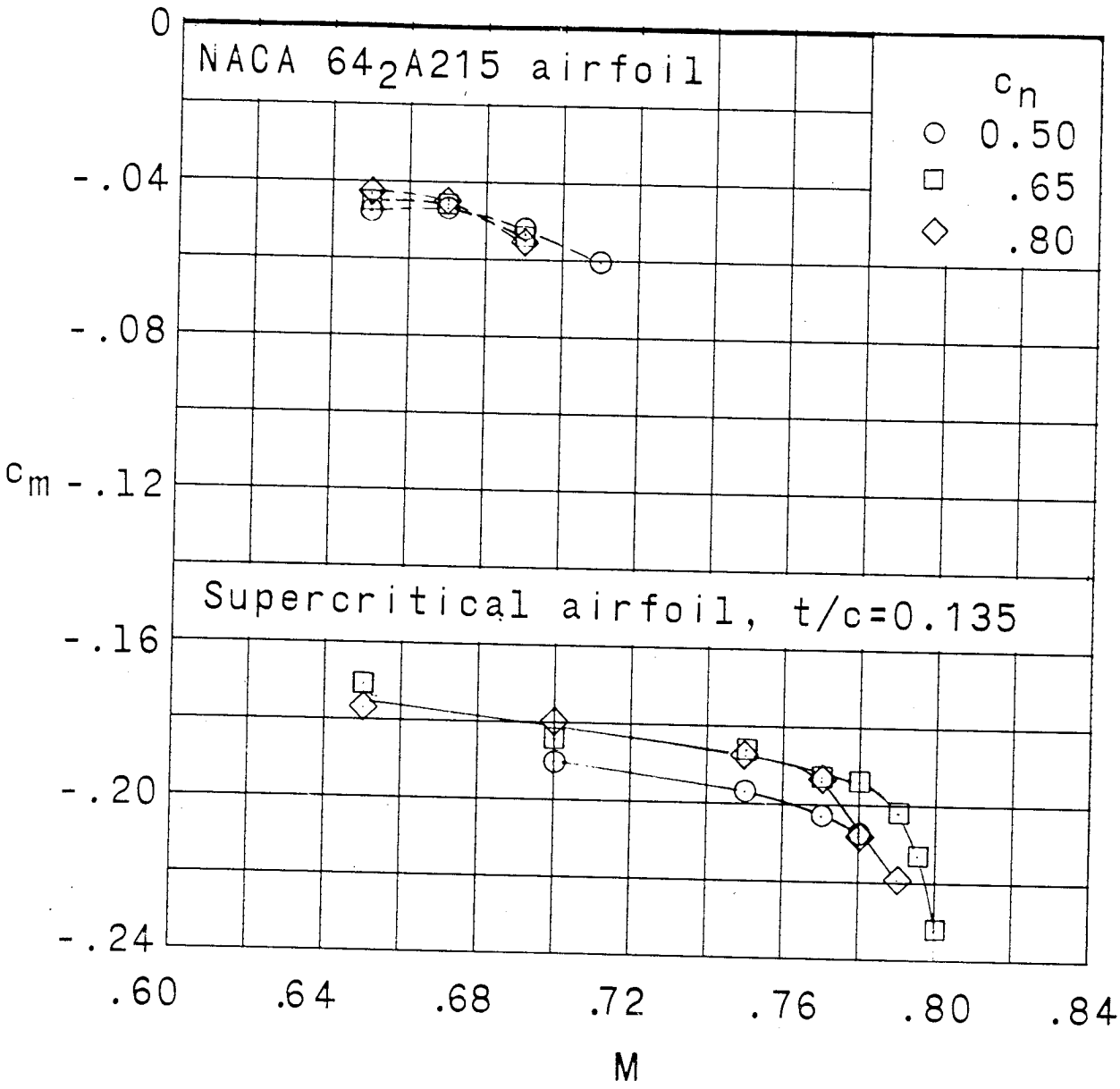

(c) Pitching moment.

Figure 7.- Concluded.

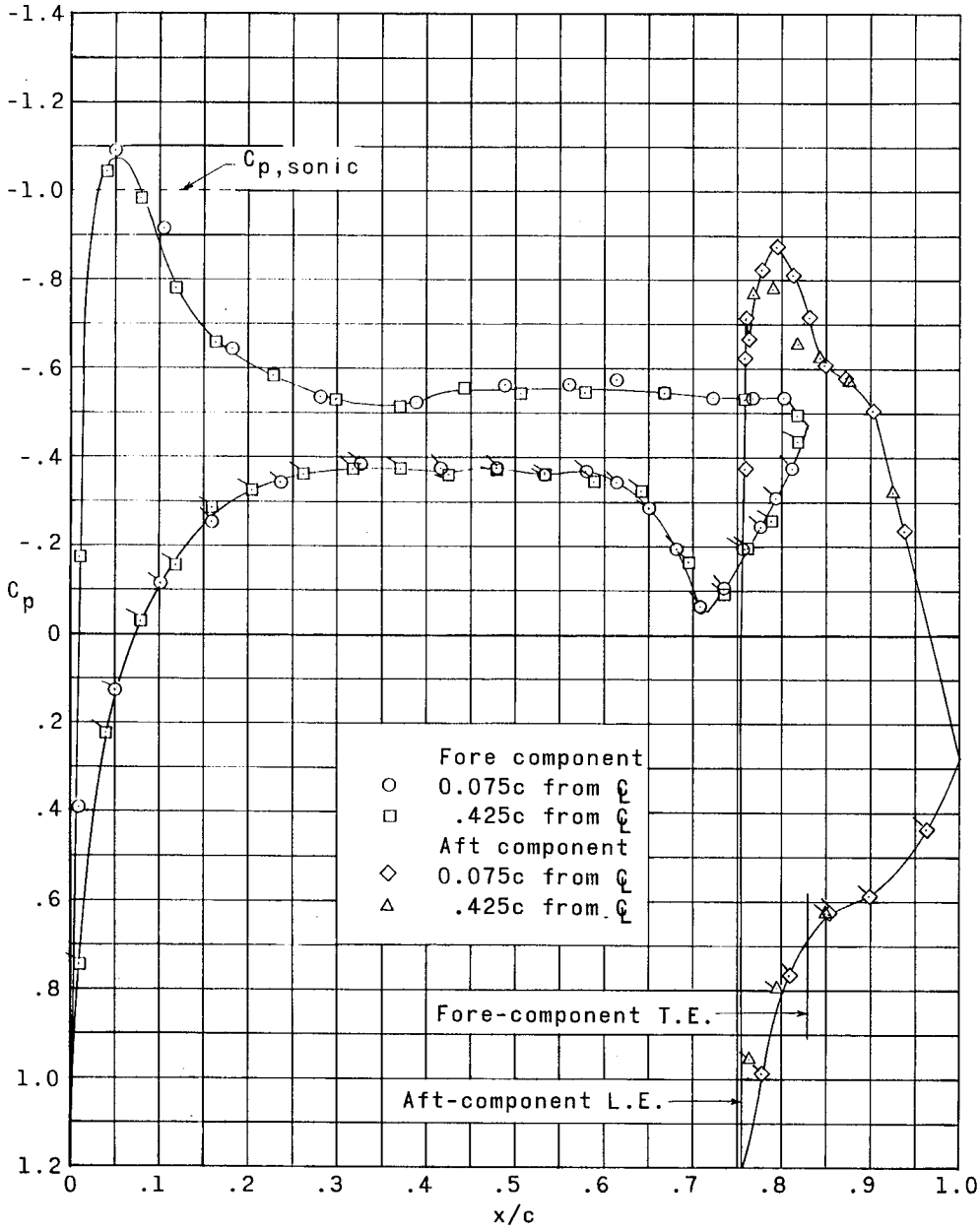

(a) M = 0.65.

Figure 8.- Pressure distributions and schlieren photographs for supercritical airfoil. $\alpha = 0^{\circ}$. (Flagged symbols for lower surface values.)

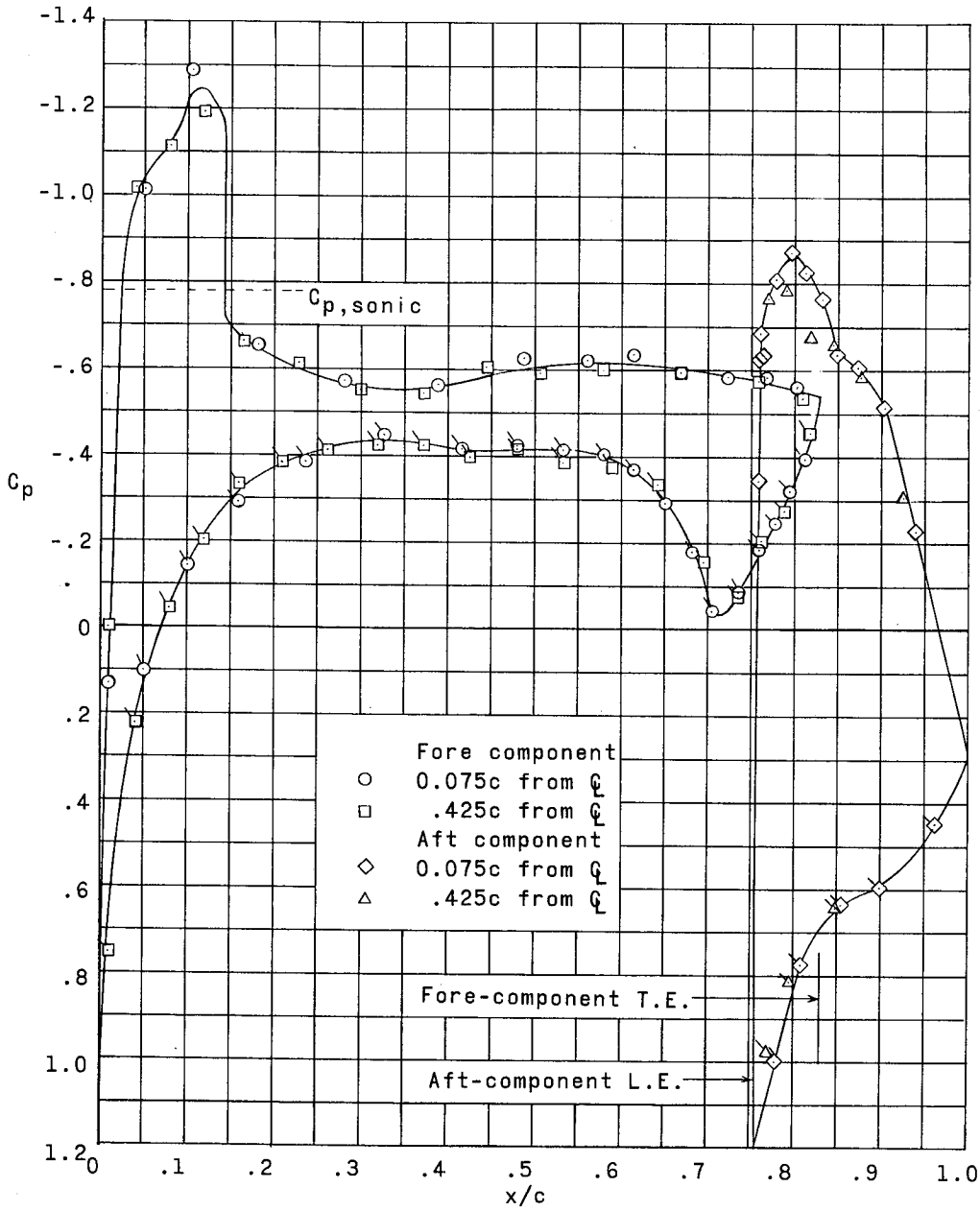

(b) M = 0.70.

Figure 8.- Continued.

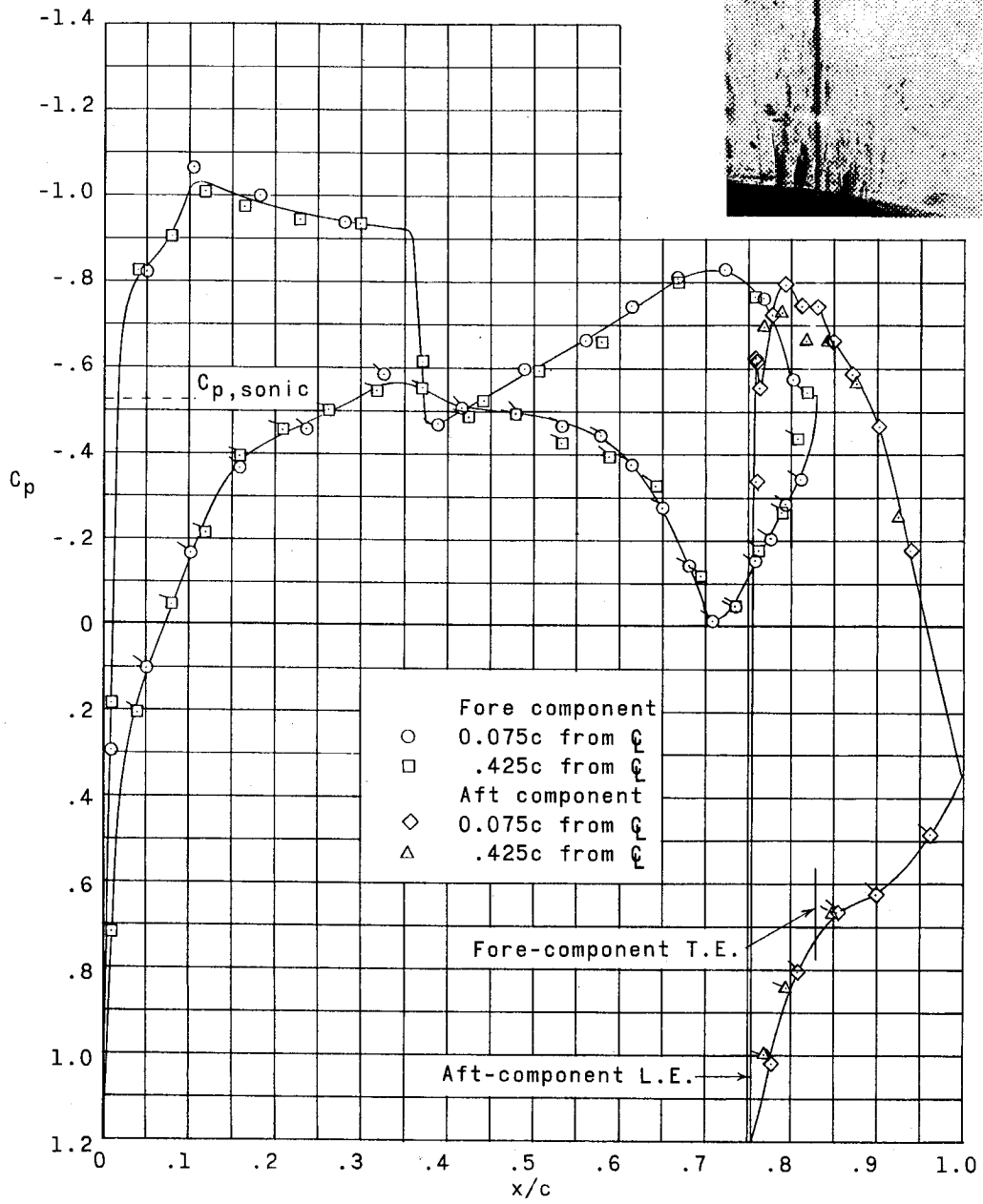

(c) M = 0.77. L-65-96

Figure 8.- Continued.

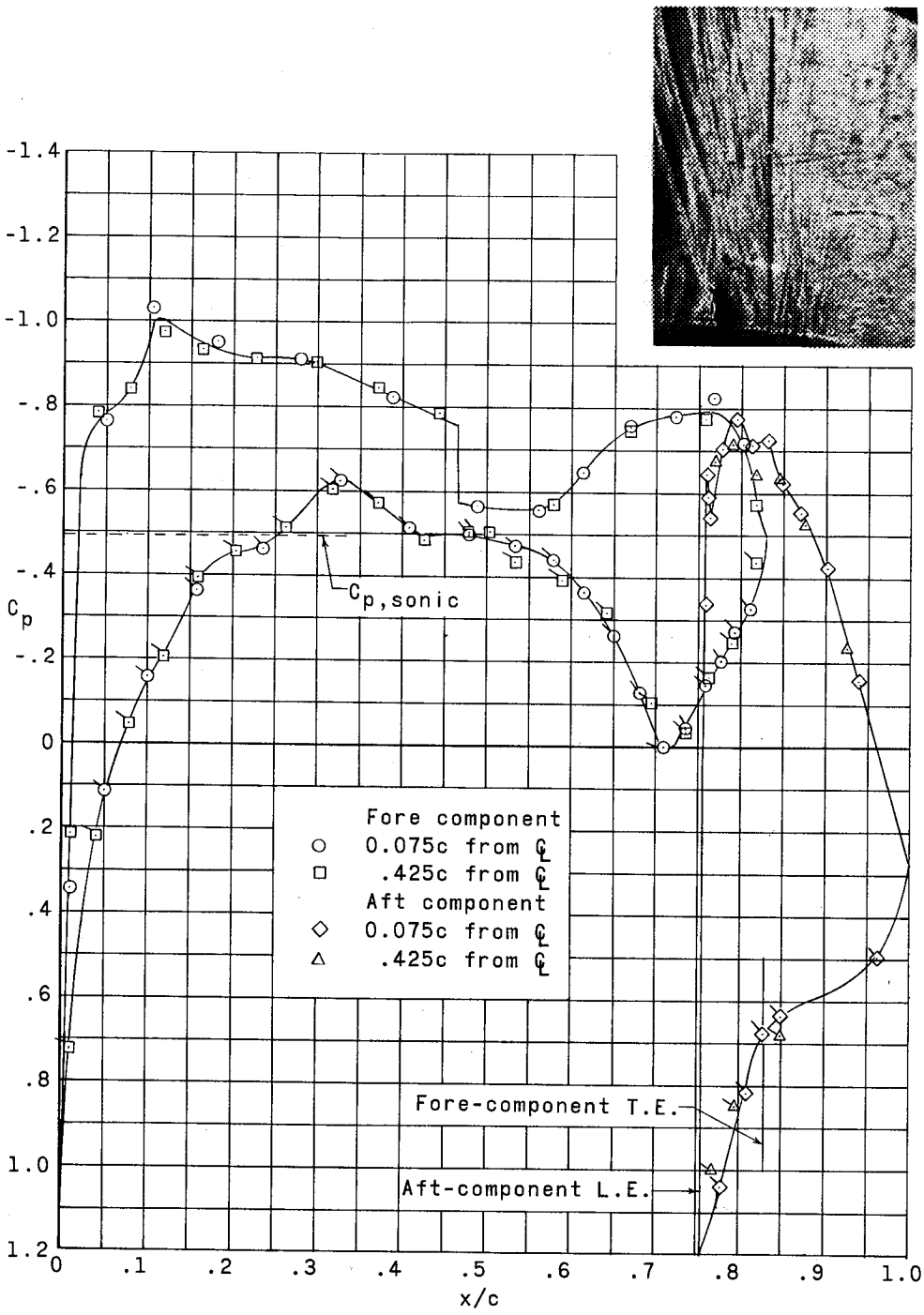

(d) M = 0.78. L-65-97

Figure 8.- Continued.

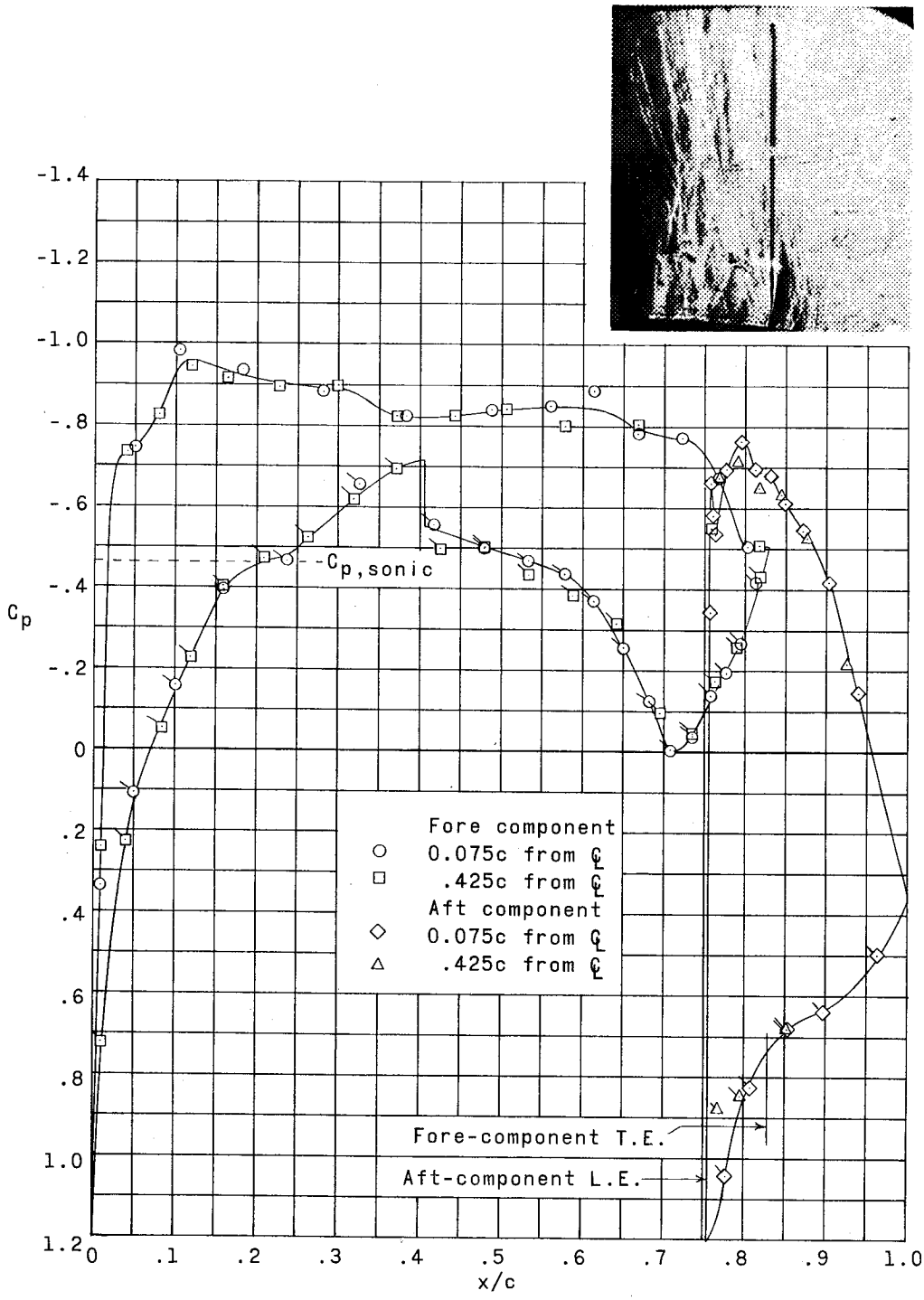

(e) M = 0.79.

L-65-98

Figure 8.- Continued.

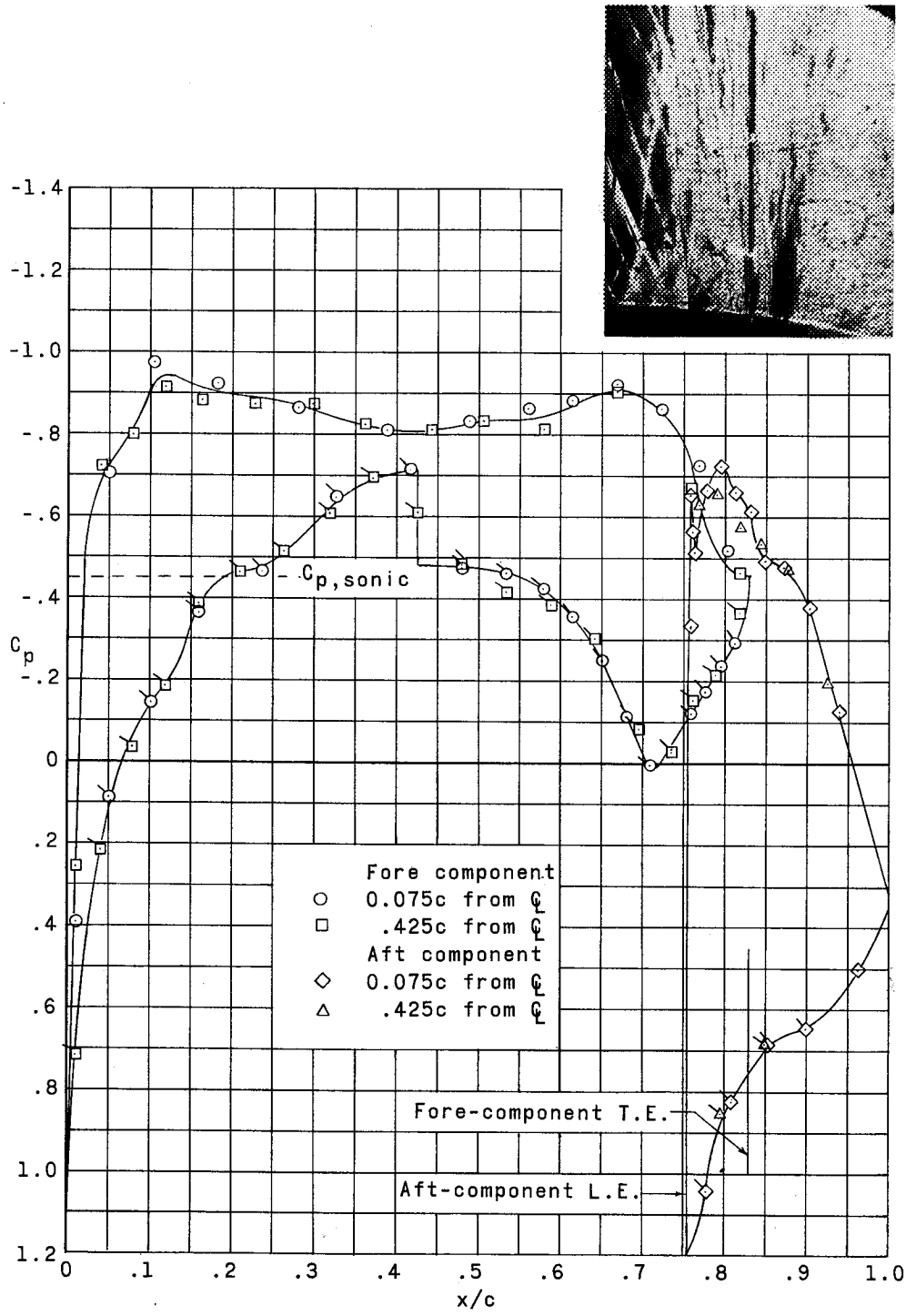

(f) M = 0.795. L-65-99

Figure 8.- Continued.

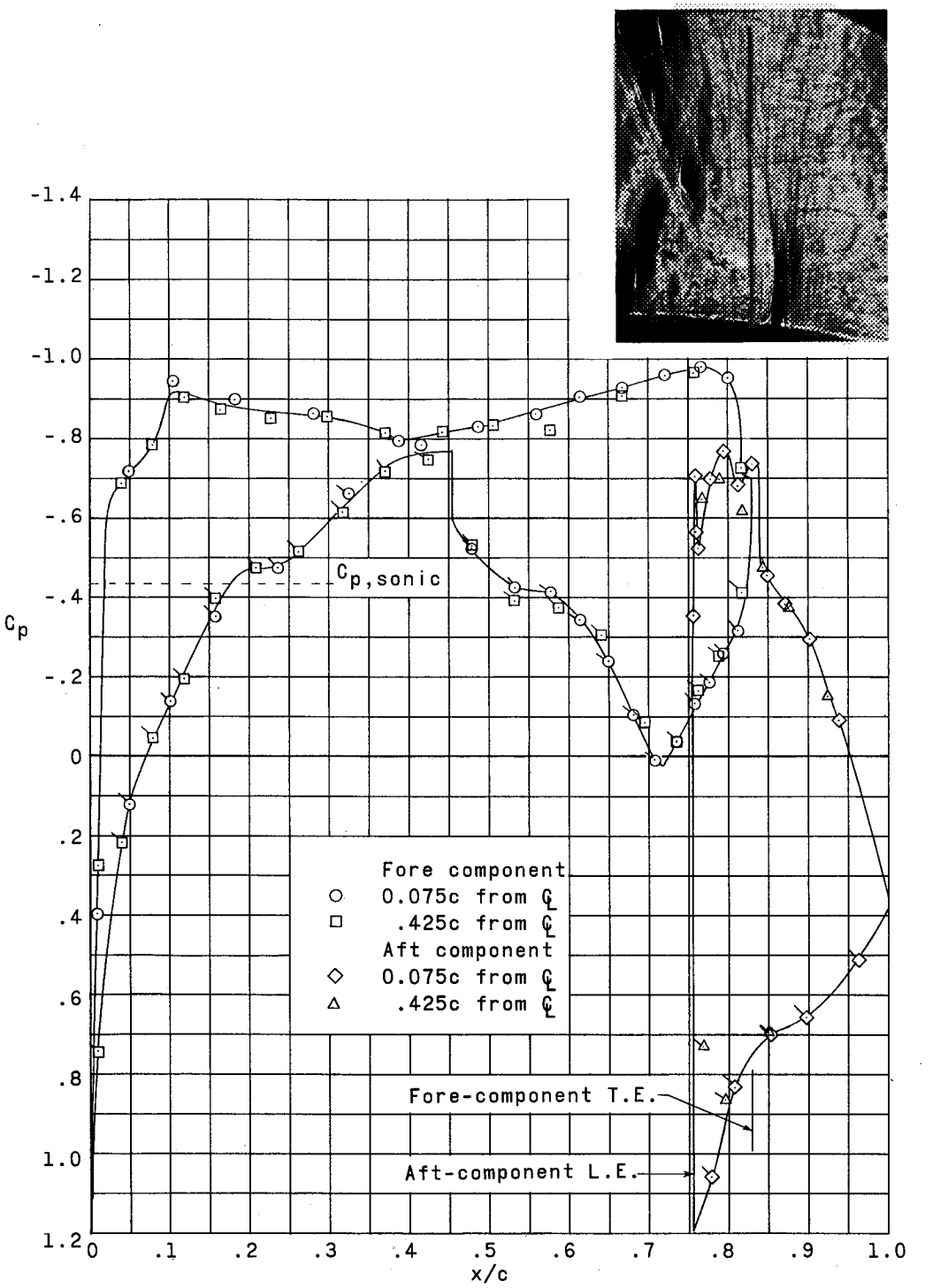

(g) M = 0.80. L-65-100

Figure 8.- Concluded.

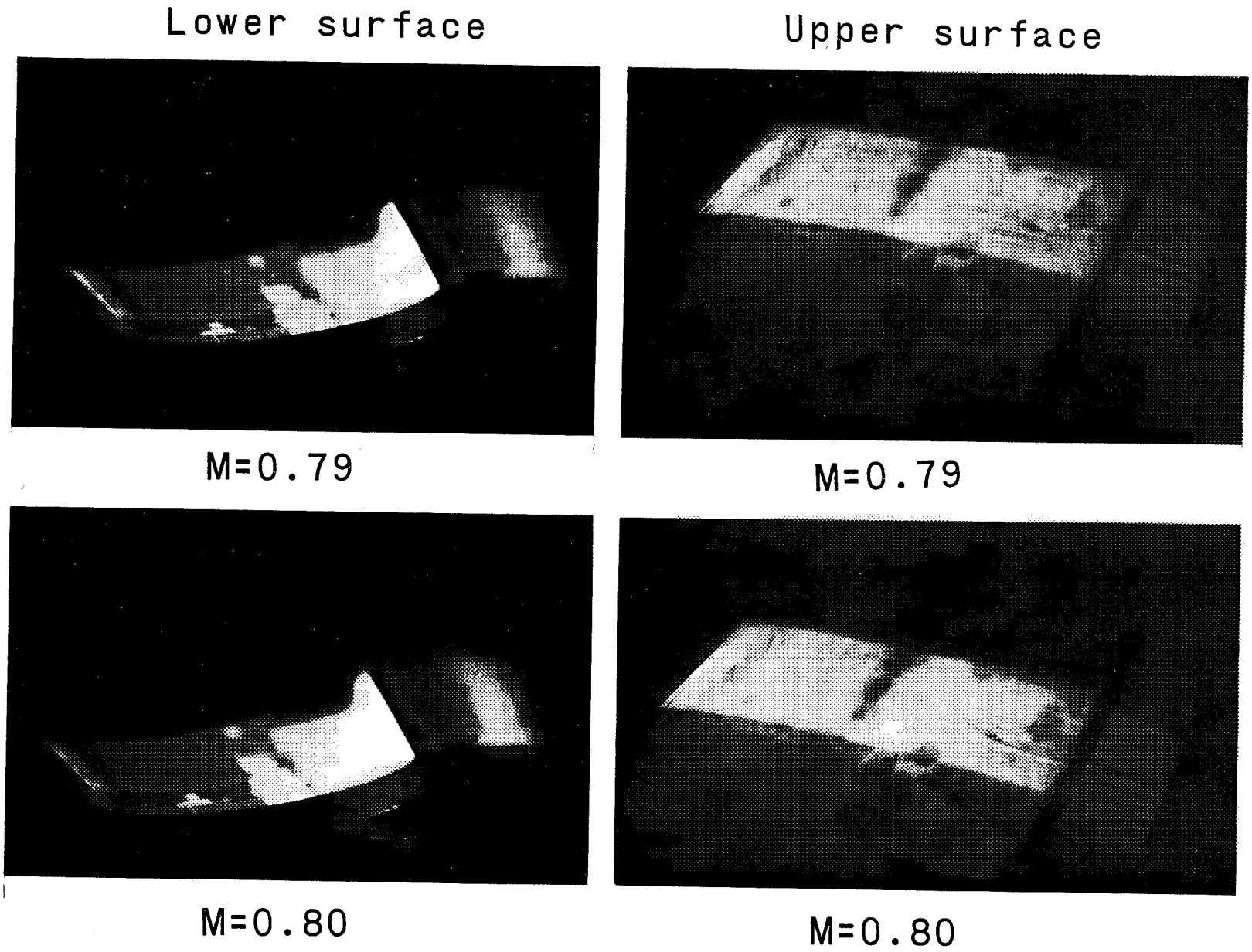

Figure 9.- Photographs of surface oil flow on supercritical airfoil. $\alpha = 0^{\circ}$. L-65-101

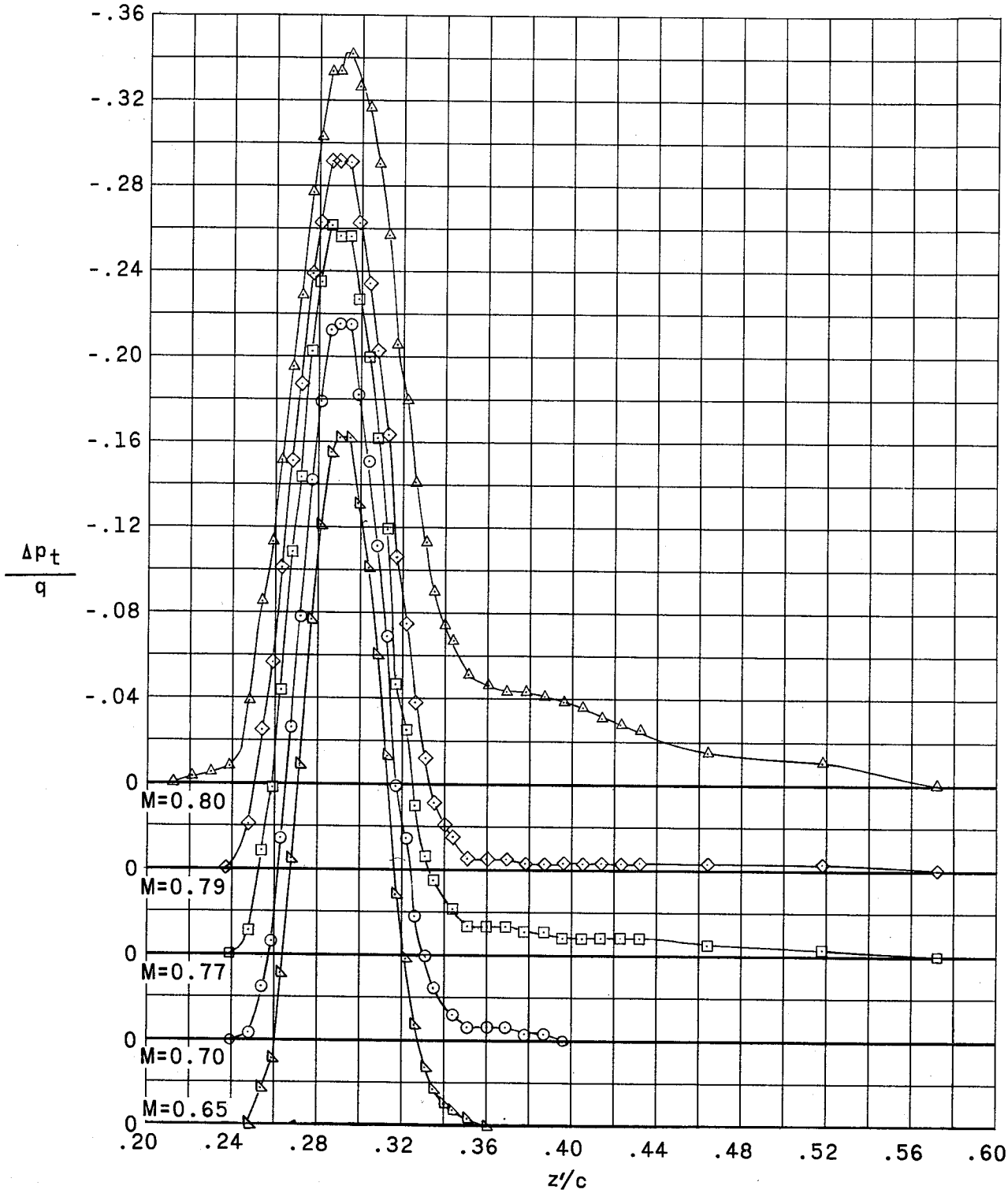

Figure 10.- Wake profiles for supercritical airfoil. $\alpha = 0^{\circ}$.

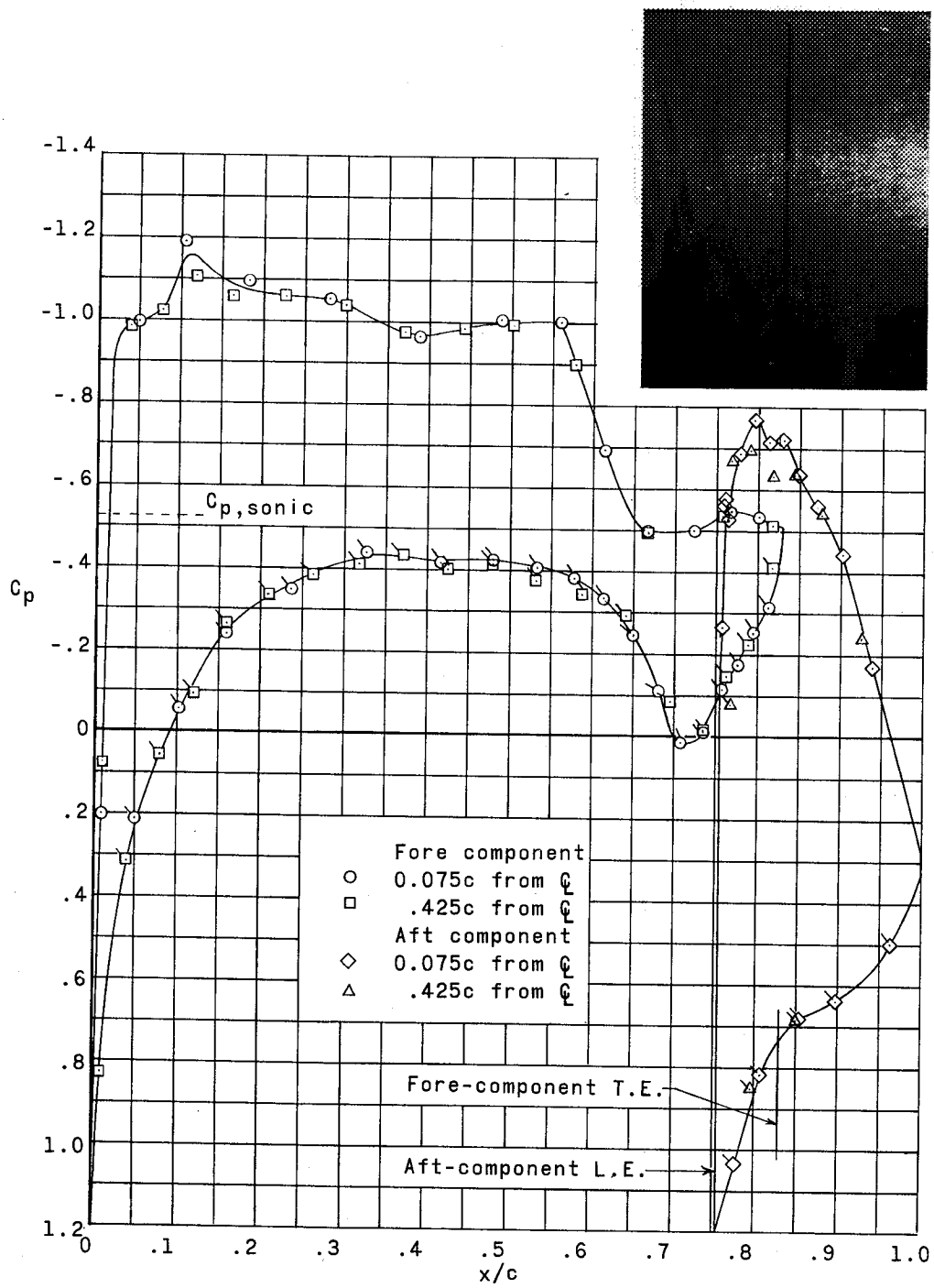

L-65-102

Figure 11.- Pressure distributions and schlieren photographs for supercritical airfoil; $\alpha = 1^{\circ}$, M = 0.77. (Flagged symbols for lower surface values.)

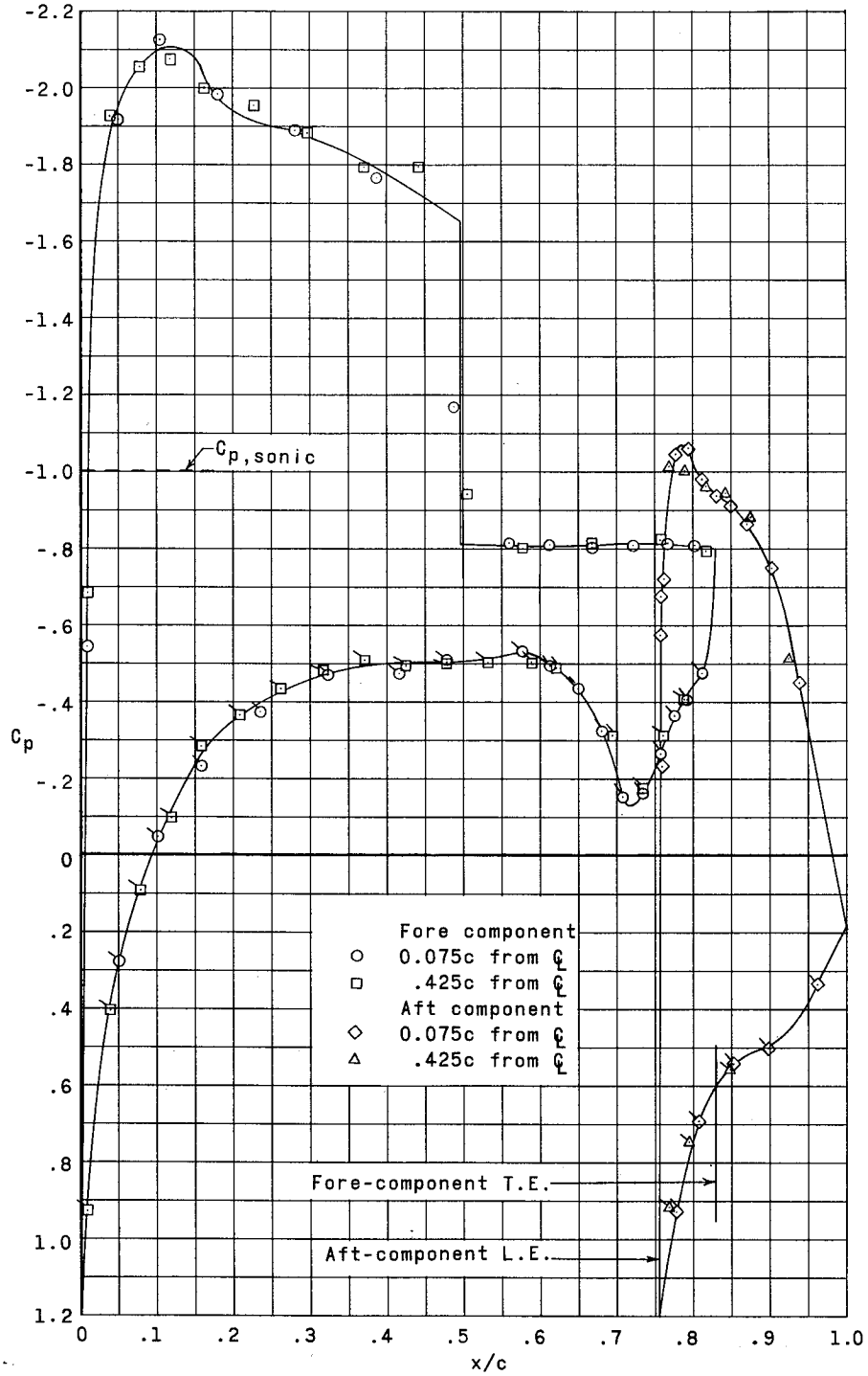

(a) M = 0.65.

Figure 12.- Pressure distributions for supercritical airfoil. $\alpha = 3^{\circ}$. (Flagged symbols for lower surface values.)

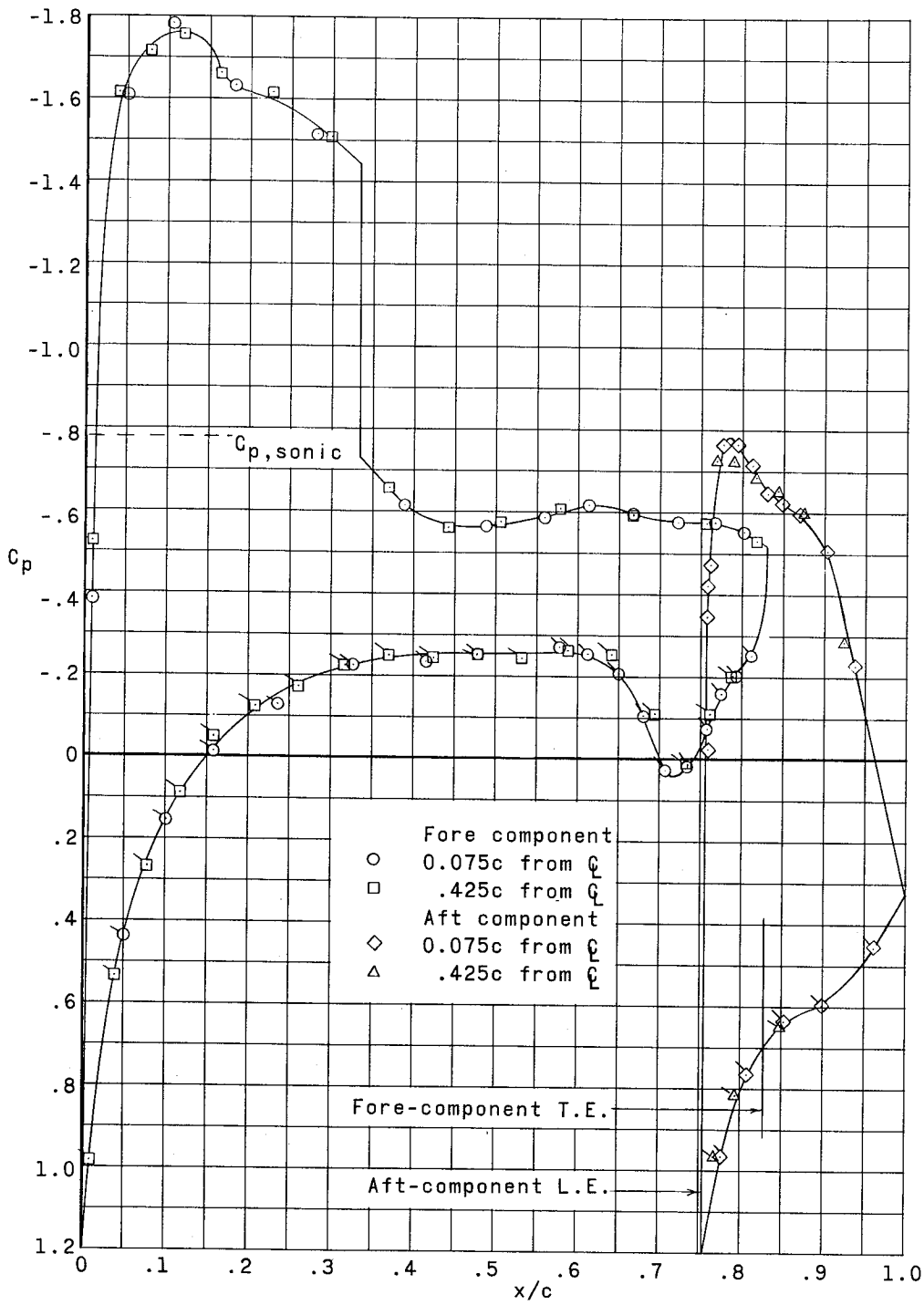

(b) M = 0.70.

Figure 12.- Continued.

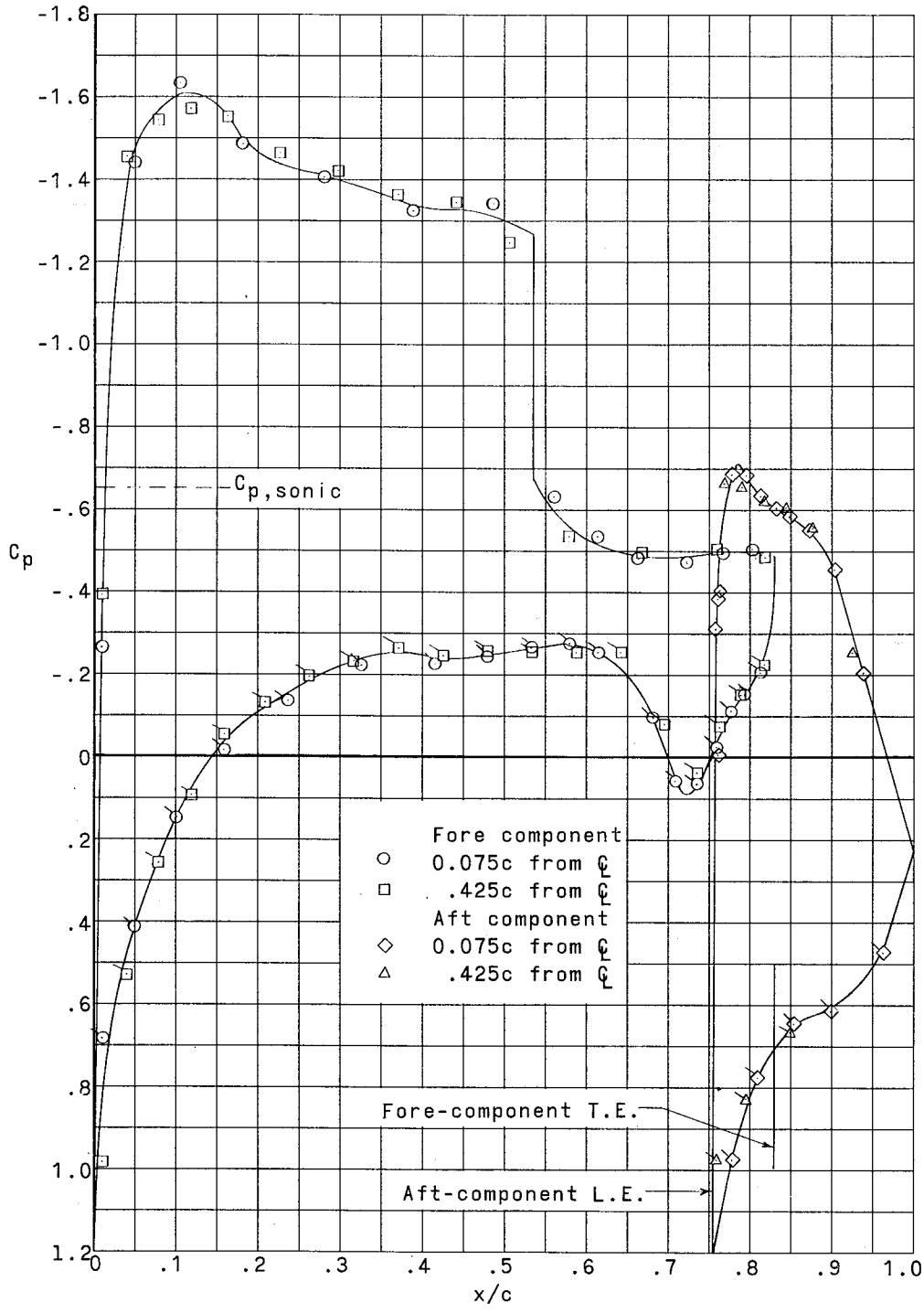

(c) M = 0.73.

Figure 12.- Continued.

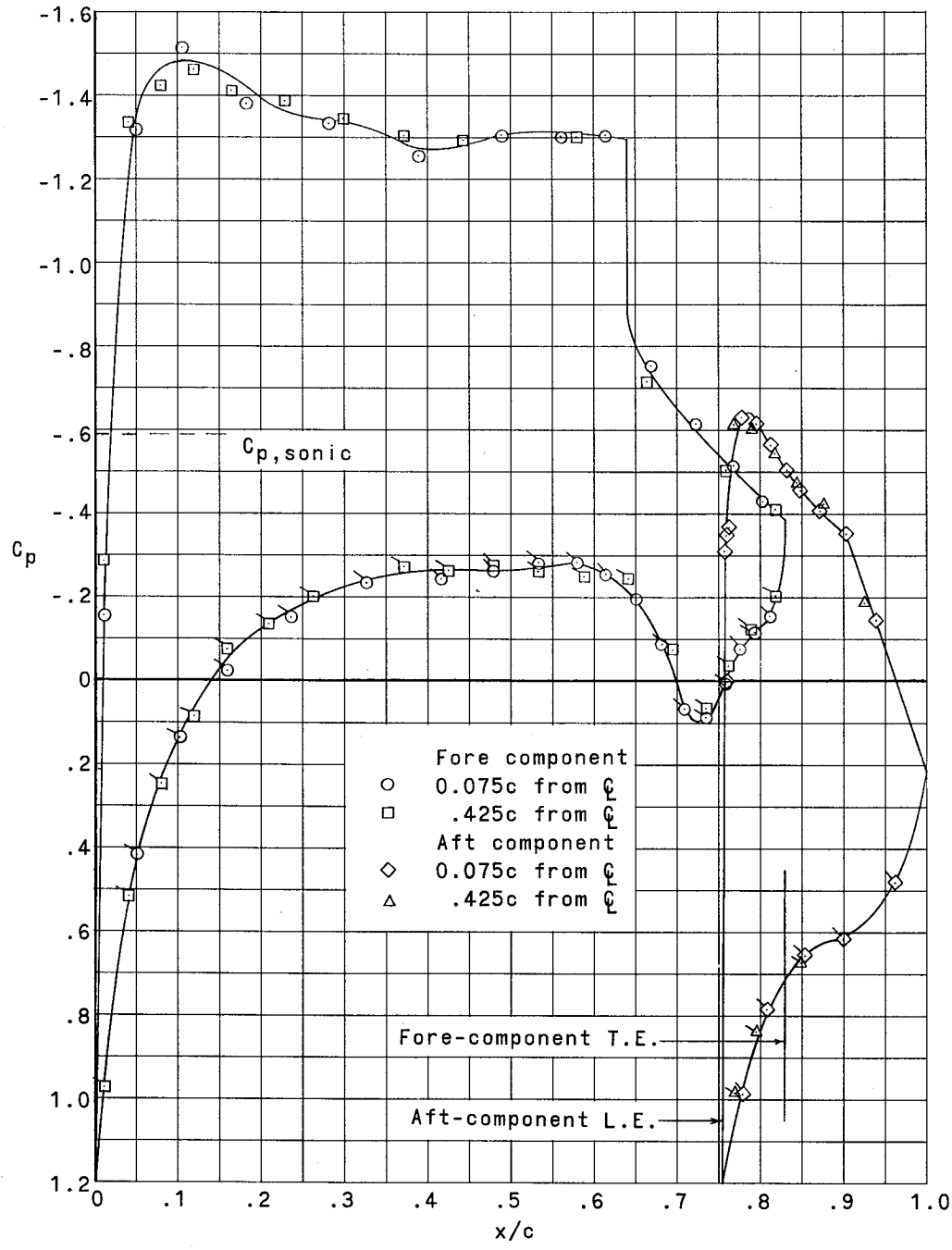

(d) M = 0.75.

Figure 12.- Concluded.

M=0.65

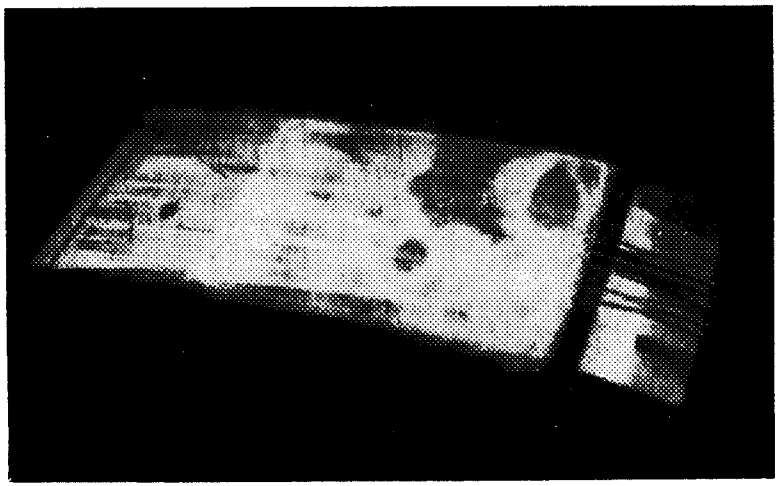

M=0.70

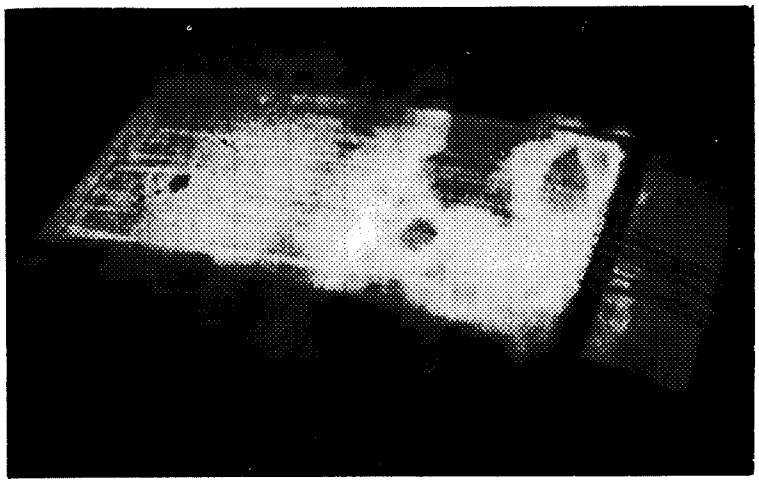

M=0.73

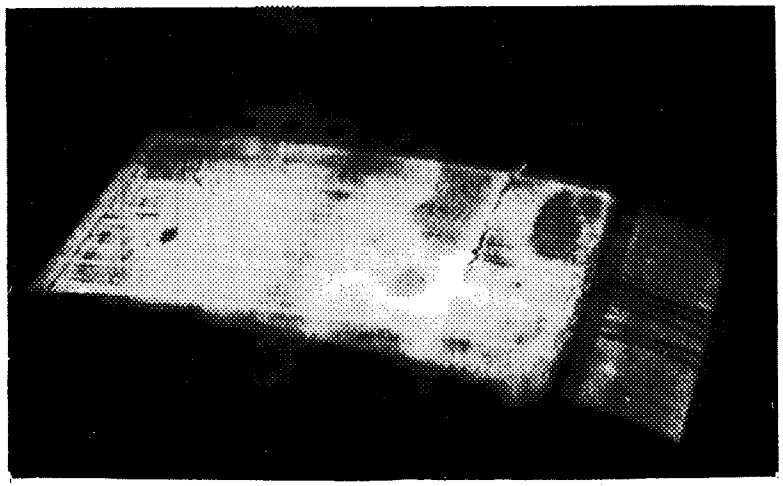

M=0.75

Figure 13.- Photographs of surface oil flow on upper surface of supercritical airfoil. $\alpha = 3^{\circ}$. L-65-103

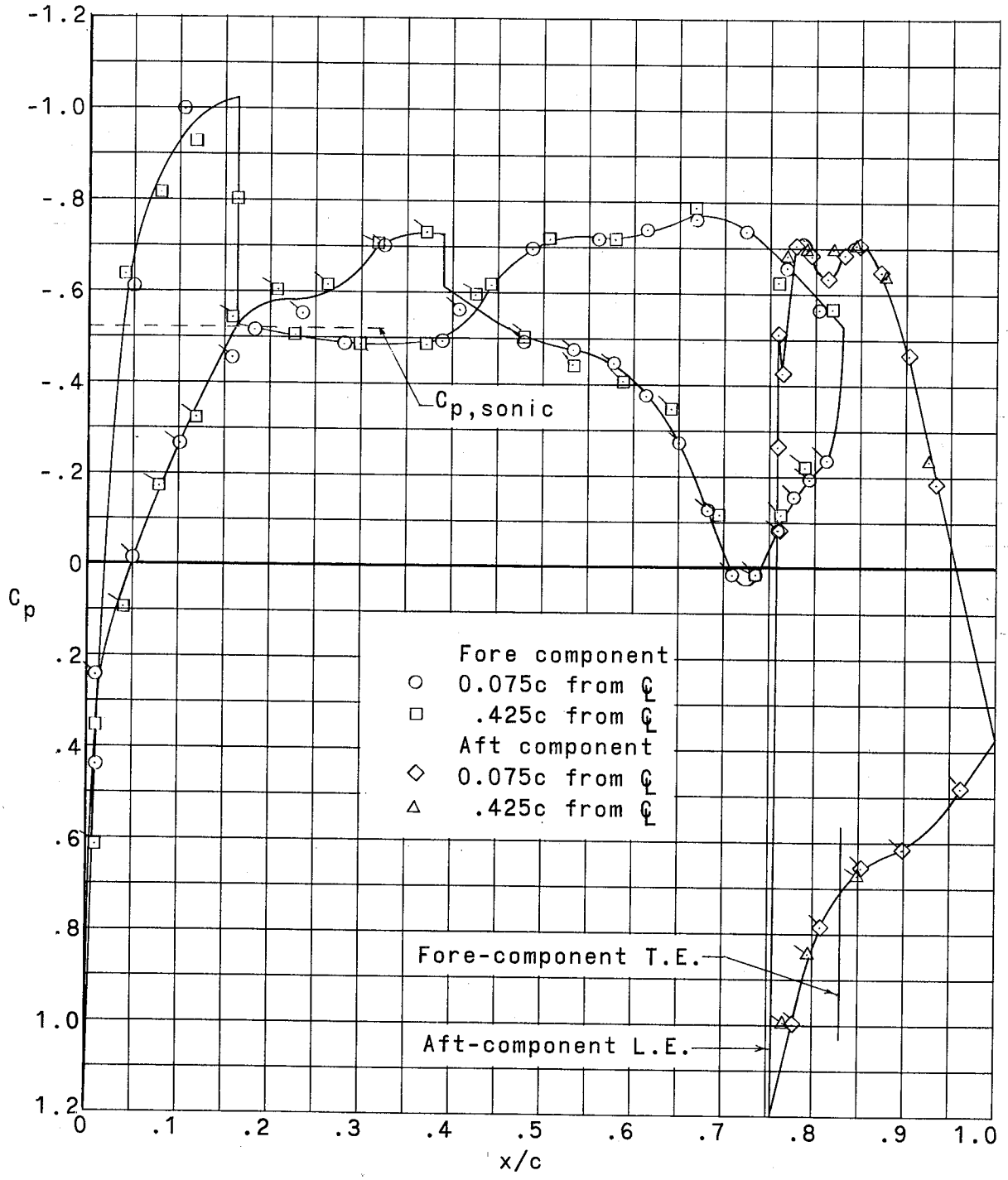

(a) M = 0.77.

Figure 14.- Pressure distributions for supercritical airfoil. $\alpha = -1^{\circ}$.
(Flagged symbols for lower surface values.)

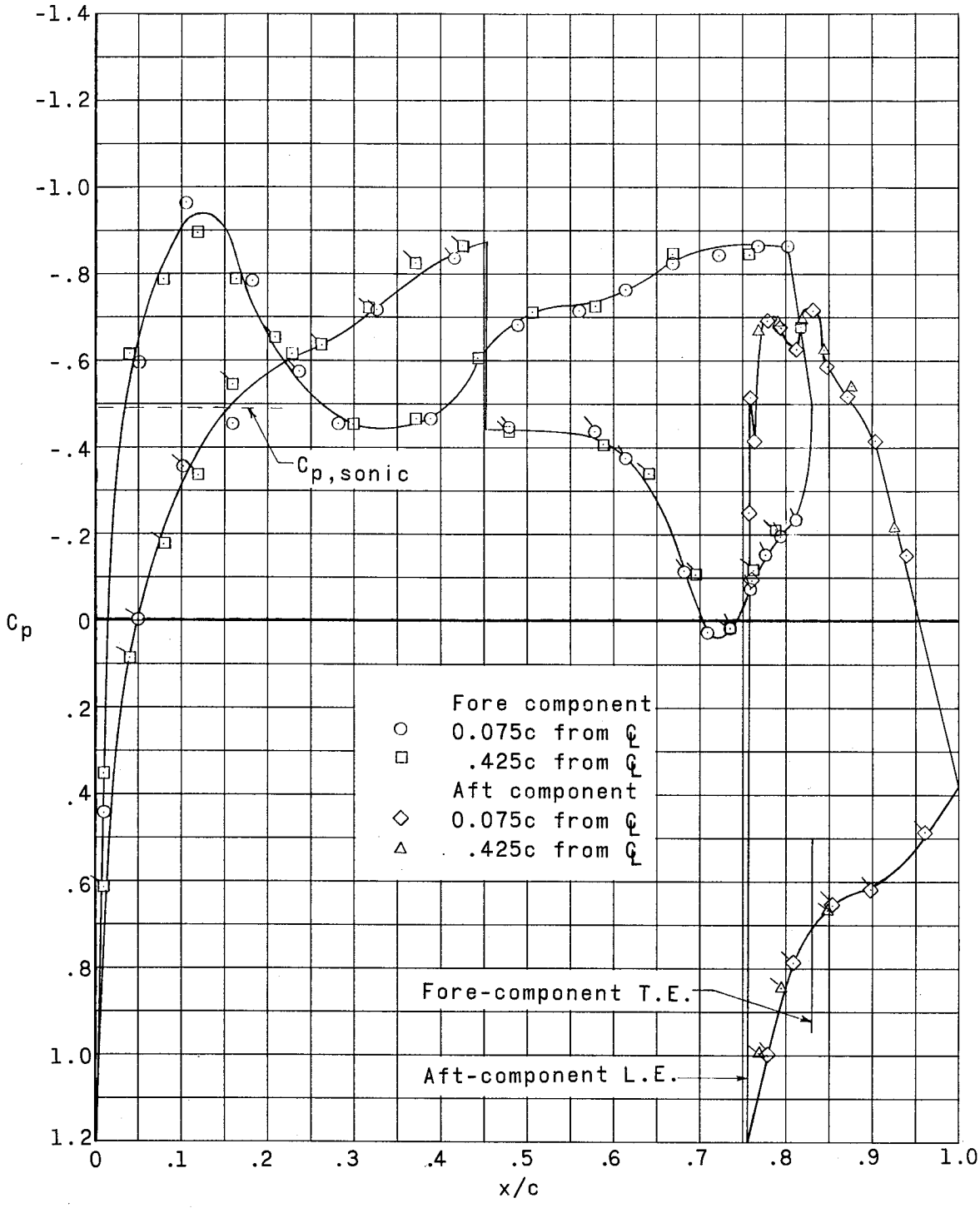

(b) M = 0.78.

Figure 14.- Concluded.